Space Sci Rev (2020) 216:1
https://doi.org/10.1007/s11214-019-0619-5

Quiescent Discrete Auroral Arcs: A Review of Magnetospheric Generator Mechanisms

Joseph E. Borovsky[1] · Joachim Birn[1] · Marius M. Echim[2,3] · Shigeru Fujita[4,5] · Robert L. Lysak[6] · David J. Knudsen[7] · Octav Marghitu[3] · Antonius Otto[8] · Tomo-Hiko Watanabe[9] · Takashi Tanaka[10]

Received: 10 June 2019 / Accepted: 12 November 2019

Abstract One of the longstanding questions of space science is: How does the Earth's magnetosphere generate auroral arcs? A related question is: What form of energy is extracted from the magnetosphere to drive auroral arcs? Not knowing the answers to these questions hinders our ability to determine the impact of auroral arcs on the magnetospheric system. Magnetospheric mechanisms for driving quiescent auroral arcs are reviewed. Two types of quiescent arcs are (1) low-latitude non-Alfvénic (growth-phase) arcs magnetically connecting to the electron plasma sheet and (2) high-latitude arcs magnetically connecting near the plasma-sheet boundary layer. The reviews of the magnetospheric generator mechanisms are separated for the two types of quiescent arcs. The driving of auroral-arc currents in large-scale computer simulations is examined. Predicted observables in the magnetosphere and in the ionosphere are compiled for the various generator mechanisms.

Keywords Aurora · Magnetosphere · Plasma physics · Discrete arcs

Auroral Physics
Edited by David Knudsen, Joe Borovsky, Tomas Karlsson, Ryuho Kataoka and Noora Partmies

✉ J.E. Borovsky
jborovsky@spacescience.org

1 Center for Space Plasma Physics, Space Science Institute, Boulder, CO, USA

2 Institut Royale d'Aeronomie Spatiale de Belgique, Bruxelles, Belgium

3 Institute of Space Science, Bucharest, Romania

4 Meteorological College, Kashiwa, Japan

5 National Institute of Polar Research, Tachikawa, Japan

6 School of Physics and Astronomy, University of Minnesota, Minneapolis, MN, USA

7 Department of Physics and Astronomy, University of Calgary, Calgary, Alberta, Canada

8 Geophysical Institute, University of Alaska, Fairbanks, AK, USA

9 Department of Physics, Nagoya University, Nagoya, Japan

10 International Center for Space Weather Science and Education, Kyushu University, Fukuoka, Japan

Published online: 16 December 2019

1 Introduction

The mechanisms that generate auroral arcs are not fully understood; neither is the form of energy conversion that occurs when the arc is powered by the magnetosphere. In various models the energy powering the auroral arc comes from magnetic-field energy, ion pressure, electron pressure, flow kinetic energy, solar-wind-driven waves, etc. For magnetospheric physics the generation of auroral arcs by the magnetosphere has been an outstanding question for decades, as testified in the reviews of auroral-arc generator mechanisms (e.g. Swift 1978; Atkinson 1978; Borovsky 1993; De Keyser and Echim 2010; Haerendel 2011). (For a review of pre-space-age theories of the cause of aurora, see Eather 1980.)

An auroral arc is a geomagnetic east-west aligned curtain of optical emission in the upper atmosphere produced by the impacts of magnetospheric electrons that were accelerated downward along the Earth's magnetic field. The emission is associated with an east-west aligned sheet of upward magnetic-field-aligned electrical current that connects into the magnetosphere, with the current carried largely by the downward-accelerated electrons.

The purpose of this review is to discuss contemporary ideas about the magnetospheric generators of quiescent auroral arcs: what mechanisms provide the power for the arcs, what mechanisms divert the current from the magnetosphere, what mechanisms produce the perpendicular electric fields and related E-cross-B flows. By "quiescent" we mean arcs not associated with dynamic events such as substorm breakup, and which have lifetimes ranging from several minutes to hours. These quiescent arcs are typically associated with electron energies of keV to tens of keV. Because they may be driven by different magnetospheric processes, quiescent arcs are split into two types in this review: (1) high-latitude quiescent arcs magnetically connected to the plasma sheet boundary layer (PSBL) and associated with Alfvén waves in the magnetosphere and/or with magnetospheric interfaces (e.g. Burke et al. 1994; Keiling et al. 2006) and (2) low-latitude quiescent arcs magnetically connected into the electron plasma sheet and associated with mild geomagnetic activity prior to substorm onsets ("growth-phase arcs") or without substorms occurring (Feldstein and Galperin 1985; Galperin and Feldstein 1996; Motoba et al. 2015). Low-latitude field-line-resonance (FLR) arcs (e.g. Samson et al. 1996; Gillies et al. 2017), which also are associated with Alfvén waves, are not discussed in this review.

Auroral arcs do not necessarily have a one-to-one relation to upward current sheets; in some cases single or multiple arcs are current-sheet intensifications within broader regions of upward field-aligned current (Wu et al. 2017). Growth-phase quiescent arcs have optical widths of 0.2–30 km (Kim and Volkman 1963; Knudsen et al. 2001; Partamies et al. 2010), often appear in multiple sets (Akasofu 1976; Wu et al. 2017), and can appear simultaneously in conjugate hemispheres (Sato et al. 1998; Motoba et al. 2012) but favor the winter hemisphere (Newell et al. 1996a). Auroral arcs are associated with geomagnetic activity: the stronger the activity (and the strong the solar-wind driving), the more intense the auroral-arc activity (Sandford 1968; Newell et al. 2009). Auroral arcs are associated with perpendicular electric fields (Marklund 1984) and with vorticity (flow shear) (Kelley and Carlson 1977). During very quiet times, discrete arcs can be absent, though it is believed that some level of auroral emission is essentially always present somewhere. The properties of quiescent discrete auroral arcs are reviewed in Karlsson et al. (2019).

From a systems science point of view, auroral arcs can be considered to be an "emergent phenomenon" in the magnetosphere-ionosphere system (Borovsky and Valdivia 2018). As such, understanding how an arc is produced might require a global (e.g. whole-magnetotail) discussion. Because of their energy extraction, the emergence of arcs has an impact on the system behavior.

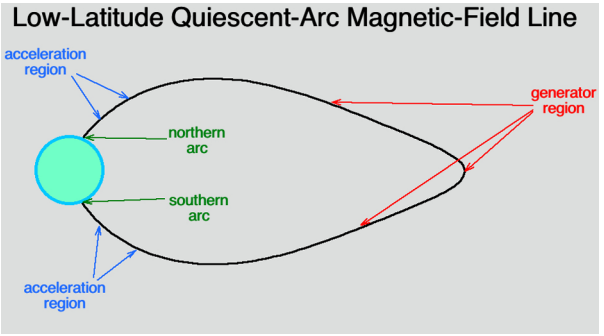

Fig. 1 A sketch of the magnetic-field line connecting a quiescent arc in the atmosphere to the plasma sheet in the nightside magnetosphere

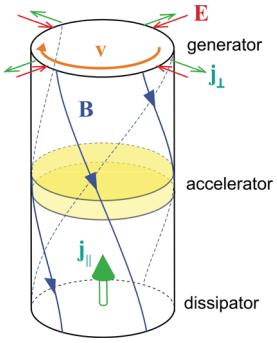

Fig. 2 A simplified sketch of the field, currents, and flows of an auroral arc (in an idealized cylindrical geometry for illustrative purposes) showing the generator region, an accelerator region, and a dissipator region. Magnetic fields are in blue, currents are in green, and electric fields are in red. (Cf. Fig. 3.7.c of Paschmann et al. 2002)

The arc is the site of intense energy extraction from the magnetosphere, with the magnetospheric energy powering the electron acceleration and the flow of current in the dissipative ionosphere. An auroral arc can be envisioned (see Fig. 1) as being comprised of three key regions that are magnetically connected: (1) a generator region in the magnetosphere that supplies power and current to the arc, (2) an accelerator region above the ionosphere where magnetospheric electrons are accelerated downward toward the Earth, and (3) an ionospheric dissipation region that contains the atmospheric-emission curtain.

Figure 2 illustrates these regions in the simplest, cylindrically symmetric, form for the fields and currents that are typically associated with an arc. (1) The generator region in the magnetosphere consists of a shear flow or twisting motion associated with a converging electric field. During a buildup phase this causes a magnetic shear or twist of a magnetic flux tube, corresponding to an increase of upward field-aligned current. For long lasting arcs this would lead into a steady state. By current continuity, the field-aligned current must become converted into (or from) perpendicular current $j_\perp$ in the magnetosphere, with $j_\perp$ being opposite to the electric field, thus constituting the generator ($\underline{J} \bullet \underline{E} < 0$). (This perpendicular current that feeds the field-aligned current is associated with a field-aligned gradient of the field-aligned vorticity Song and Lysak 2006.) The perpendicular electric field together with the perturbed azimuthal magnetic-field component also provide the downward Poynting flux that powers the arc. (2) The perpendicular electric field is known to be stronger at high altitudes than near the ionosphere (Weimer et al. 1985); in a quasi-static state this implies an upward electric field parallel to $\underline{B}$ in the acceleration region, which causes the electron acceleration. In the acceleration region this also represents a load ($\underline{J} \bullet \underline{E} > 0$), which converts part of the power. The parallel electric field may also be visualized as a partial field line slippage, which reduces the twisting motion. (3) In the ionosphere, the field-aligned current

is again closed through perpendicular current, which together with the remaining perpendicular electric field (and corresponding motion) represents a load ($\underline{J} \bullet \underline{E} > 0$), which now causes dissipation via Ohmic heating.

This simple cylindrical picture, however, needs to be modified in light of several facts. One is the geometry of an arc, which is strongly elongated in the east-west direction in the ionosphere (cf. Hallinan 1981). In the magnetosphere, this may be associated with a geometry in which the electric field, associated with the shear motion, may be aligned in one direction, but the current diversion is in the transverse direction. And the vectors need not be collocated. Also in the magnetotail, the perturbed currents that connect to the field-aligned currents are superposed onto unperturbed currents, particularly the cross tail current, which distorts the generator and load picture. Furthermore, the current diversion and generator regions, which appear closely connected in the simple picture of Fig. 2, may be separated substantially, as found in MHD simulations to be discussed in Sect. 5.

The simple picture of Fig. 2 also leaves out the ultimate energy source in the magnetosphere. While the twisting or shear motion appears to be essential this does not mean that the energy is supplied by the kinetic motional energy. Most detailed energy release and conversion investigations in magnetotail models and observations have found a strong dominance of enthalpy (that is, essentially thermal energy) flux (Birn and Hesse 2005; Aunai et al. 2011; Eastwood et al. 2013; Tyler et al. 2016). But how and where this is converted to the Poynting flux that eventually powers the arcs is still uncertain. The picture illustrated in Fig. 2 applies not only to ion or plasma flows but also, on smaller scales potentially relevant for arcs, to electron flows.

Determining the generator mechanism of low-latitude quiescent auroral arcs (and the impact that those arcs have on the magnetosphere) is hindered by uncertainties as to where the visible arcs map to in the nightside magnetosphere. One school has low-latitude arcs magnetically connected into the plasma sheet in the outer dipolar portion of the nightside magnetosphere (e.g. McIlwain 1975; Meng et al. 1979; Kremser et al. 1988; Elphinstone et al. 1991; Pulkkinen et al. 1991; Mauk and Meng 1991; Lu et al. 2000; Yang et al. 2013; Motoba et al. 2015), a second school has those arcs magnetically connected to the plasma sheet in the stretched magnetotail (e.g. Yahnin et al. 1997, 1999; Birn et al. 2004a,b, 2012; Sergeev et al. 2012; Hsieh and Otto 2014), and a third school has the low-latitude arcs magnetically connected into the mid magnetotail but with the arc current generated at the plasma-sheet/lobe boundary (e.g. Tanaka 1995, 2015; Tanaka et al. 2017; Ebihara and Tanaka 2017). In mapping quiescent auroral arcs into the nightside magnetosphere, it is unlikely that they magnetically connect to the equatorial region of the magnetotail beyond about 15 R_E: even under quiet geomagnetic conditions those regions of the plasma sheet are characterized by turbulent flow (Borovsky et al. 1997; Voros et al. 2007; Stepanova et al. 2011; El-Alaoui et al. 2012) and irregular magnetic field (Borovsky and Funsten 2003; Voros et al. 2004). An example is given in Fig. 3 where the flow and field measured at $X = -20$ R_E are shown for an interval of normal geomagnetic activity. It is difficult to see how a laminar, large-scale quiescent arc could be driven from such an irregular dynamic region.

This review is organized as follows. Section 2 reviews generator mechanisms for high-latitude quiescent arcs associated with the plasma sheet boundary layer: Sect. 2.1 discusses arcs driven by Alfvén waves and Sect. 2.2 discusses arcs driven by plasma interfaces. Section 3 reviews generator mechanisms for low-latitude quiescent arcs: Sect. 3.1 reviews the driving of arcs by pressure gradients in the plasma sheet, Sect. 3.2 reviews an arc model based on plasma pressure and magnetic stress in the global magnetospheric convection, Sect. 3.3 reviews arcs that are driven by thin current sheets in the Earth's plasma sheet, Sect. 3.4 reviews the stationary-Alfvén-wave picture of arcs driven by magnetic energy, and Sect. 3.5 reviews ionospheric-feedback models for auroral arcs. Section 4 discusses the

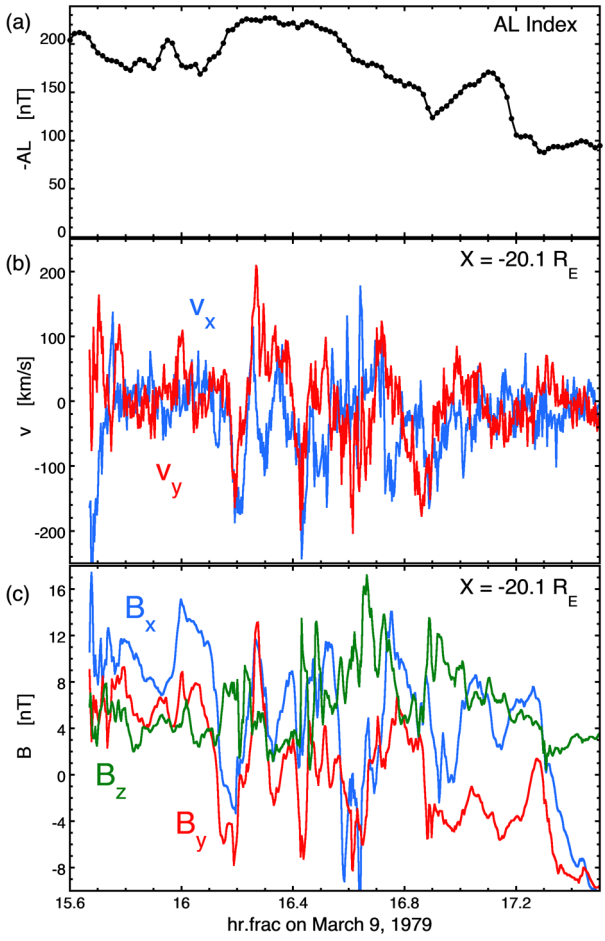

Fig. 3 ISEE-2 measurements in the plasma sheet 20 R_E downtail. Average value of -AL for years 1966–2013 is 128 nT

driving of arcs located near the Harang discontinuity. Section 5 looks at what large-scale numerical simulations say about the driving of quiescent auroral arcs. Section 6 summarizes the review and provides an overview of unknown issues associated with the generation of quiescent auroral arcs. A number of arc-generator models from the literature that are in disuse are briefly discussed in the Appendix.

2 High-Latitude Quiescent Arcs: The PSBL and LLBL

High-latitude quiescent auroral arcs have been associated with the polar-cap boundary and plasma sheet boundary layer (PSBL) (e.g. Burke et al. 1994; Onsager and Mukai 1996). On the duskside, these arcs might be consistent with magnetic connection into the low-latitude boundary layer (e.g. Echim et al. 2008). High-latitude quiescent arcs tend to involve the precipitation of lower-energy electrons than do low-latitude arcs (Boyd et al. 1971; Safargaleev et al. 2003; Karlsson et al. 2019)

In equilibrium models of the magnetotail (in GSE coordinates), the Y-direction magnetic-field flaring of the plasma sheet is larger than the Y-flaring of the lobe magnetic

field (cf. Fig. 4 of Birn 1989 or Fig. 1 of Birn and Hesse 1991): this means that there is a magnetic shear between the lobe and the plasma sheet, and a Region-I sense field-aligned current associated with that magnetic shear. At $X = -100$ R_E, the plasma sheet flares about 5 R_E further in the Y direction than the lobe does (cf. Figs. 2–5 of Birn and Hesse 1991). This means that the magnetic shear angle is about 5/100 radians, or about 2.9° at this downtail distance. If the magnetic-field strength is about 20 nT, then the change in B_y from the lobe to the plasma sheet is about 1.0 nT, which corresponds to a field-aligned current per unit length $J_\parallel = 8 \times 10^{-4}$ A/m in the shear, where the length is in the Y-direction. At $X = -100$ R_E, the premidnight shear layer is about 20 R_E in extent in the Y-direction (cf. Figs. 2–5 of Birn and Hesse 1991), giving a total field-aligned current in the PSBL shear layer of 1×10^5 A going into one hemisphere. For a 15-km-wide high-latitude arc at the PSBL with an energy flux of 20 mW/m^2 carried by 3 keV electrons (numbers from Vaivads et al. 2003), the current of the arc is 1×10^5 A if the arc is 1000-km long in the ionosphere. In a sense, the high-latitude quiescent arc is part of the equilibrium configuration of the magnetotail.

The Earth's low-latitude boundary layer (LLBL) also magnetically connects to the high-latitude portion of the auroral oval near the polar-cap boundary, although the connection may be predominantly to the dayside ionosphere (e.g. Elphinstone et al. 1991). The velocity shear between the tailward-moving flow of the LLBL relative to the more-stationary plasma sheet has a vorticity $\underline{\omega} = \nabla \times \underline{v}$ in the equatorial plane that has $\underline{\omega} \bullet \underline{B} > 0$ on the dusk side of the Earth, which corresponds to a negative space charge (cf. Eq. (11) of Borovsky and Birn 2014) and converging perpendicular electric fields as in auroral arcs. And on the dusk side the twist of the magnetic field produced by the tailward flow of the LLBL relative to the plasma sheet corresponds to a field-aligned current that is out of the ionosphere: a Region-I sense current as is the current associated with the PSBL. This mapping is pertinent to the model discussed in Sect. 2.2.

2.1 Alfvén-Wave-Driven Arcs

Alfvén-wave Earthward Poynting flux is seen for these high-latitude arcs (e.g. Wygant et al. 2000; Chaston et al. 2003; Keiling et al. 2006). Time-varying Alfvén waves with small perpendicular scale sizes (a few km or less in the auroral zone) are able to accelerate electrons to energies as high as few keV (Goertz and Boswell 1979; Lysak and Song 2011) and in transient bursts ($\sim$ 1 s in duration) as high as 10 keV (Watt and Rankin 2010). While these spatial and temporal scales are at or below the low end of those relevant to quiescent arcs, Alfvén waves are involved in the transient stage leading to quiescent arcs, and may be important in maintaining "red-line" arcs produced by lower-energy electrons (Gillies et al. 2017; Liang et al. 2019). In a generator-accelerator-ionosphere picture of the arc (cf. Fig. 4), the Alfvén waves play the role of the accelerator: to determine the magnetospheric cause (generator) of the arc, one must determine what drives the Alfvén waves near the PSBL and where the energy for the waves comes from.

Zelenyi et al. (2004) and Grigorenko et al. (2007) have argued that the Alfvén waves (which have linear polarizations with the wave's velocity and magnetic-field vectors in the Y direction in the magnetotail) are driven by firehose instabilities powered by Earthward-traveling beams of energetic ions in the PSBL, known as velocity dispersed ion beams (e.g. Takahashi and Hones 1988; Zelenyi et al. 1990). Since the gradients in the beam intensity are stronger in the Z direction than the Y direction it was argued (Zelenyi et al. 2004; Grigorenko et al. 2007) that the firehose would produce the observed Y-direction polarization of the Alfvén waves. In this picture, the source of the ion beams is the source (generator) of the arc. If the Earthward ion beams are produced by Earthward plasma flow from magnetotail

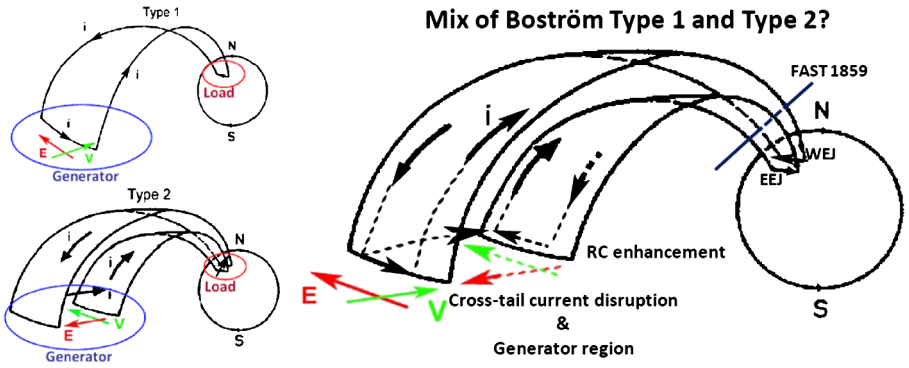

Fig. 4 Left: Type 1 and Type 2 auroral current circuit. Adapted after Boström (1964). Right: Mix of Type 1 and Type 2 (see text). Figure based on Marghitu et al. (2009) and on subsequent FAST and Swarm work on longitudinal gradients in the auroral region, as yet unpublished

reconnection process (e.g. Onsager et al. 1991; Birn et al. 2015), then the energy source of the high-latitude Alfvénic arc is magnetic-field annihilation associated with the distant reconnection site. If the Earthward ion beams are produced by Speiser-orbiting ions escaping from the cross-tail current sheet (e.g. Lyons and Speiser 1982; Bosqued et al. 1993) then the beams have obtained their energization in a cross-tail electric field, which is consistent with a coherent large-scale convection in the magnetotail. In the turbulent regions of the magnetotail (Borovsky et al. 1997; Voros et al. 2004; Weygand et al. 2005) beyond $\sim 15\ R_E$ where Earthward transport is dominated by bursty bulk flows (Angelopoulos et al. 1993, 1994; Cao et al. 2013) and where the electric field is spatially and temporally chaotic (Cattell and Mozer 1982; Pedersen et al. 1985; Borovsky et al. 1998a), the concept of a global cross-tail electric field may not be valid.

It has been argued (Wright and Allan 2008) that if there were a source of fast magnetosonic-mode waves in the plasma sheet (such as from a substorm or the movement of a reconnection plasmoid), the fast mode waves could mode convert into shear Alfvén waves in the plasma sheet boundary layer; similarly it has been argued (Dmitrienko 2011) that fast magnetosonic waves entering the magnetotail from the solar wind could mode convert into shear Alfvén waves in the plasma sheet boundary layer. To make a quiescent high-latitude arc during quiet geomagnetic times, the magnetosonic-wave source in the solar wind is more promising than is the (impulsive) source in the plasma sheet. This is similar to the idea that solar-wind-driven Kelvin-Helmholtz waves on the magnetotail magnetopause could mode convert into shear (and kinetic) Alfvén waves in the plasma sheet boundary layer (Smith et al. 1986; Harrold et al. 1990; Hanson and Harrold 1994) (see also Ruderman and Wright 1998). In these pictures, the power source for the arc is the solar-wind driving wave energy into the magnetotail.

Another potential source of shear Alfvén waves in the PSBL is associated with distant reconnection and the flaring of the magnetotail. As noted above, in the equilibrium configuration of the magnetotail there is a change in flaring angle between the open field lines of the lobes and the closed field lines of the plasma sheet, with a Region-I sense field-aligned current at the PSBL. As a northern-lobe magnetic-field line reconnects at the distant X line, it convects downward in Z to join the plasma sheet. The Z velocity of the field line and its plasma is approximately 0.1 v_A for collisionless reconnection (Birn et al. 2001), where v_A is the local Alfvén speed at the reconnection site. Owing to the change in flaring angle between magnetic-field lines in the lobe and magnetic-field lines in the plasma sheet, the field

line and its plasma must also flow in the Y-direction outward from local midnight after it crosses the separatrix. With the plasma carried on the field line, this Y flow will have some inertia. If the inertia carries the field line past the equilibrium flaring angle of the plasma sheet, there may be a $v_y - B_y$ spatio-temporal oscillation set up in the Z flow entering the PSBL from the lobe (i.e. in the PSBL). This oscillation will take the form of a shear Alfvén wave, with the linear polarization as observed for Alfvén waves in the PSBL (Wygant et al. 2000). Whether or not there is an Alfvénic oscillation will depend on how rapidly the field line makes the transition in flaring angle.

Although not for a quiescent arc, Lysak et al. (2009) have pointed out that the Earthward plasma injection from a near-Earth neutral line at substorm onset compresses plasma and launches fast-mode waves that can propagate from the equatorial region of the plasma sheet to become mode converted into Alfvén waves at the PSBL to produce poleward boundary intensifications.

Electron acceleration by dispersive Alfvén waves is limited to velocities of less than 2 v_A (Kletzing 1994), corresponding to energies of less than ~ 2 keV, and resulting in relatively dim emissions dominated by the red line. Furthermore, Alfvénic acceleration is inherently transient, which makes it seemingly incompatible with quiescent arcs, although the long lifetime of red-line emissions will tend to smooth out dynamical variations. Therefore, Alfvén waves may explain electron acceleration within low-energy arcs such as high-latitude (PSBL) arcs. They also clearly play a role in field-line resonance arcs, which occur most frequently at dawn and at dusk (Gillies et al. 2018), in contrast to the brighter and more energetic growth-phase arcs that are most common near midnight.

2.2 Model of Magnetospheric Interface Driven Quiescent Arcs: PSBL and LLBL

Motivated by the works of Lyons et al. (1979), Lyons (1980, 1981) and Lyons and Evans (1984), Roth et al. (1993) suggested that magnetospheric plasma interfaces provide the electromotive force needed to sustain the magnetic-field-aligned potential difference that accelerates auroral electrons. One key feature is the polarization electric field across the plasma interface sustained by pressure gradients or shears of bulk velocity. Roth et al. (1993) portray this magnetospheric DC generator with an analogy to the "contact potential" difference produced at the interface between two metallic conductors at different temperatures" and show examples of kinetic Vlasov solutions computed for interfaces formed in the Earth's plasma sheet. The ultimate energy of the coupled auroral arc is provided by the polarization electric field across the generator. This polarization electric field is stronger when the temperature and/or density gradient, and/or the velocity shear across the plasma interface is stronger.

Roth et al. (1996), Echim et al. (2007, 2008), De Keyser and Echim (2010, 2013), De Keyser et al. (2010) further developed these ideas and evaluated qualitatively and quantitatively the auroral effects due to the magnetic coupling between the strong electric fields formed at magnetospheric interfaces and the auroral ionosphere. It is argued that plasmas with different macroscopic properties (e.g. density, temperature, bulk velocity) are in contact in various regions of the magnetosphere (e.g. at the inner edge of the Low Latitude Boundary Layer (LLBL) or the Plasma Sheet Boundary Layer (PSBL)) and lead to the formation of transition layers/interfaces with scale lengths of the order of the electron and/or proton gyroradius or larger. Extensive earlier work focused on the driving of arcs by the velocity shear between the plasma sheet and the tailward-flowing LLBL (e.g. Sonnerup 1980; Lundin and Evans 1985; Lotko et al. 1987; Wei et al. 1996).

The interaction between particles with different macroscopic properties from the two sides of the magnetospheric interface leads to electric polarization and formation of a normal electric field. A Vlasov kinetic treatment provides the profile of variation across the

interface of the plasma moments (e.g., current and charge density, temperature, bulk velocity, etc.) and of the electromagnetic field. The interface is connected to the auroral ionosphere by magnetic-field lines such that magnetospheric/ionospheric particles can move downwards/upwards in the magnetic flux tube connecting the DC generator to the auroral ionosphere. The field-aligned dynamics of these particles is affected by the magnetic mirroring and electrostatic forces. Particles from the magnetospheric interface are (locally) scattered into the loss cone by wave particle interactions sustained by inherent magnetospheric turbulence and/or instabilities due to the strong gradients across the interface. The model assumes that these magnetospheric processes are sufficiently efficient to replenish permanently the loss cone. The loss cone particles will then contribute to a field-aligned current density. The mirror force impedes the downward motion of magnetospheric electrons leading to a field-aligned variation of their current density and consequently to a $\Delta\Phi$, the field-aligned potential difference between the magnetosphere and ionosphere. The latter however will accelerate electrostatically the downgoing electrons. The mutual effect of the mirror force and electrostatic acceleration determines the energy flux of the precipitating electrons. If the electric potential varies monotonically with the field-aligned distance analytical expressions can be found for the field-aligned current density of precipitating electrons (Knight 1973; Lemaire and Scherer 1973) and for the flux of precipitating energy (Lundin and Sandahl 1978) as a function of $\Delta\Phi$.

When mapped to ionospheric altitudes these expressions give the magnetospheric inflow of particles and energy. The model of Echim et al. (2007, 2008) considers also the contributions to the net field-aligned current density due to upgoing electrons and ions and downgoing ions. At the topside ionosphere the upward field-aligned current must be compensated by (perpendicular) ionospheric currents such that the current continuity $\nabla \bullet \underline{j} = 0$ is satisfied. The precipitating flux of electrons, the field-aligned current density, and the magnetospheric electrostatic potential (Φ_m) mapped to the ionospheric altitude have a spatial variation imprinted by the profile of plasma parameters and fields in the DC generator in the magnetosphere. The current continuity is the mathematical kernel that allows the computation of Φ_i, the ionospheric electrostatic potential as a function of the coordinate normal to the discrete auroral arc. It is then straightforward to compute $\Delta\Phi = \Phi_i - \Phi_m$ and all the auroral arc parameters that depend on it, like the field-aligned current density, the influx of precipitating energy, and the Pedersen conductance (see Fig. 5). The multiplicity of arcs can occur when the velocity shears and/or kinetic pressure gradients across the interface are so strong that an equilibrium configuration cannot form such that the interface splits in several smaller scale interfaces—the roots of smaller scale auroral arcs (De Keyser and Echim 2013).

These models are quasi-static and relevant for stable, discrete auroral arcs. They provide the main properties of the discrete auroral arc (like thickness, field-aligned current density, flux of precipitating energy, Pedersen conductance) as a function of the DC generator strength. This quasi-static description of the arc allows for parametric studies and leads to estimation of the effects of various types of drivers on the properties of the auroral arc. For instance it was shown that increased levels of shears at the inner edge of the LLBL tend to produce brighter arcs while increased kinetic pressure gradients lead to narrower auroral structures (Echim et al. 2008). The LLBL and the PSBL are sites where cold-hot interfaces do form. Note, however, that other types of interfaces (e.g. hot-hot) can occur in various magnetospheric regions, as for instances in the plasma sheet (De Keyser and Echim 2013).

The plasma-interface generator model and its coupling with the auroral ionosphere was validated with satellite observations. Conjugate observations of the magnetospheric generator and of the auroral arc by Cluster and DMSP spacecraft (Vaivads et al. 2003) was a

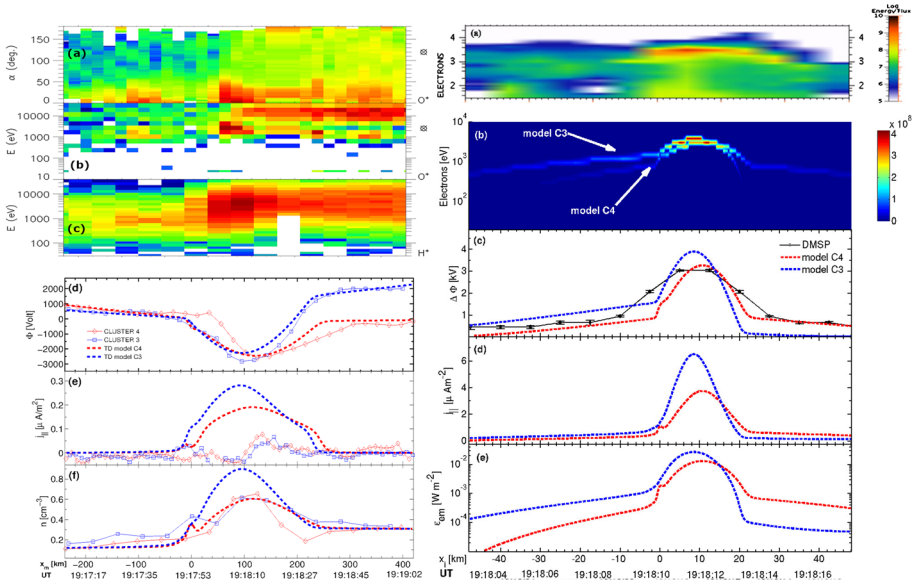

Fig. 5 The left panel shows Cluster data and model results for a magnetospheric interface generator located at the lobe-PSBL interface; (**a**) pitch angle distribution of O^+ ions, from Cluster 4 CIS (Rème et al. 2001); (**b**) O^+ and (**c**) H^+ energy spectrum from Cluster 4; (**d**) electrostatic potential from Cluster data (Vaivads et al. 2003) and model, (**e**) field-aligned current density, positive for upward current, (**f**) number density. The right panel shows model results and DMSP data for the arc connected to the generator described by the left panel; (**a**) energy of precipitating electrons from DMSP-F14; (**b**) model energy spectra obtained for Maxwellian electrons injected at 4.7 R_E; (**c**) the field-aligned potential drop, $\Delta\Phi$, derived from DMSP F14 electron spectra (black symbols) and from current continuity (dashed lines); (**d**) the field-aligned current density; (**e**) the flux of precipitating energy. Figures after Echim et al. (2009)

fortunate occasion when virtually all the model observables mentioned in Table 1 could be compared with experimental data. Echim et al. (2009) showed that their model estimates well the plasma properties of the generator (the polarization electric field normal to the interface and its V-shaped profile and spatial scale, the gradients of density, temperature and the shear of the bulk velocity), as well as the properties of the coupled auroral (the thickness, the accelerating potential, the flux of precipitating energy). A comparison between the model and the optical (by TIMES spacecraft) and in-situ (by CLUSTER) observations of a polar cap arc shows that the model estimates well the thickness of the polar cap arc, the accelerating potential and the optical emission rates (Maggiolo et al. 2012). A statistical analysis of the Region 1 field-aligned currents from DMSP data (Wing et al. 2011) confirms the trends observed from the parametric study of plasma interface generator model (Echim et al. 2008): in the afternoon sector, (12–16 MLT), an increasing density gradient across the generator interface results in an increase of the field aligned current density, a decrease of the maximum field-aligned potential drop, and has little effect on the maximum of the precipitating energy flux.

3 Low-Latitude (Growth-Phase) Quiescent Arcs

In this section various ideas about the magnetospheric mechanisms that drive quiescent low-latitude arcs (a.k.a. growth-phase arcs) are reviewed. Predictions about magnetospheric observables for the various mechanisms are collected into Table 1.

Table 1 Predicted observables for the various non-Alfvénic models for quiescent auroral-arc generation: the final column denotes where the observable should be seen, in the magnetosphere (M) or ionosphere (I)

Magnetospheric-Interface-Driven Arcs	
• Polarization electric field normal to the interface	M
• V-shaped electric potential profile across the interface	M
• Gradients of density and/or temperature and/or shears of bulk velocity	M
• Total pressure equilibrium across the interface	M
• Interface scales with the Larmor scale of dominant species	M
• Arcs's field-aligned current density and the accelerating potential increase with increasing velocity shear and density gradient in the generator	M + I
• Precipitating energy flux increases with the magnetospheric velocity shear, decreases with the generator temperature gradient, shows no dependence on the density gradient	M + I
• Arc thickness related to the Larmor radius of the species dominant in the generator and on the altitude of the generator; decreases with the density gradient in the generator	M + I
Pressure-Driven Arcs	
• $(\nabla P_i + \nabla P_e) \times \nabla B$ is southward in the equatorial region	M
• $(\nabla P_i + \nabla P_e) \times \nabla B$ must be the dominant term in the current-diversion equation	M
• Arc thickness related to radial gradient scale	M + I
• $\|B\|$ change across arc (from $\nabla_r P$ pressure equilibrium or from $\nabla_r B$ in $\nabla_a P \times \nabla_r B$)	M
Embedded Arcs	
• Pressure "ledge" profile in "radial" direction	M
• $\nabla_r P \times \nabla_a B$ southward at equator	M
• Arc thickness related to pressure-ledge thickness	M + I
• Azimuthal westward flow inside arc or tailward of arc	M + I
• Normal flow through arc	M + I
• Alfvén bounce dynamics; decay times	I
Stationary Inertial Alfvén Arcs	
• Spatial oscillations of n, $j_\parallel$, electron energy, $E_\perp$	I
• Normal flow through arc	M + I
• Reduced azimuthal magnetic twist in flow exiting arc	M + I
• Growth times	I
Thin Cross-Tail-Current-Sheet Arcs	
• Arc magnetically connects to Earthward edge of cross-tail current sheet	M
• $\underline{v}_i \neq \underline{v}_e$ in the cross-tail current sheet	M
• There is a reduction of B_{mag} in the current sheet	M
• On the field lines connecting to the cross-tail sheet there is a duskward ($j_\perp$ or $E_\perp$)	M
• Across the field lines connecting to the sheet, B_{mag} is greater on the high-latitude side than the low-latitude side (dB_{mag}/dz)	M
Feedback-Instability Arcs	
• Normal flow through arc	M + I
• Spatial oscillations of $j_\parallel$ and ionospheric conductivity in accordance with models	M + I
• Growth time and temporal oscillation period compared with models	I
All Models	
• vorticity $\underline{\omega} \bullet \underline{B} > 0$	M + I
• magnetic shear from $j_\parallel$	M + I
• upflowing ions (not Alfvénic arcs)	M

3.1 Pressure-Driven Arcs

It is well known that the magnetosphere can drive field-aligned currents into the ionosphere via particle pressure gradients that are perpendicular to the magnetospheric magnetic field: this process is described by the "Vasyliunas formula" (e.g. Eq. (3.21) of Schindler and Birn 1978, Eq. (5) of Sato and Iijima 1979, Eq. (15) of Hasegawa and Sato 1979, and Eq. (12) of Strangeway 2012)

$$\begin{aligned}(1/L_{\parallel})(j_{\parallel}/B) = {} & \left(2/B^3\right)\left([\nabla P_i + \nabla P_e] \times \nabla B\right)_{\parallel} + \left(2\rho/B^3\right)\left((d\underline{v}/dt) \times \nabla B\right)_{\parallel} \\ & - \left(1/B^2\right)\left((d\underline{v}/dt) \times \nabla \rho\right)_{\parallel} + \left(\rho/B^3\right)\underline{\omega} \bullet d\underline{B}/dt \\ & + \left(\omega_{\parallel}/eB^3\right)(\nabla k_B T \times \nabla \rho)_{\parallel} + \left(\rho/B^2\right)d\omega_{\parallel}/dt, \end{aligned} \tag{1}$$

where P_i and P_e are the ion and electron pressure, B is the magnetic-field strength, ρ is the plasma mass density, and $\underline{\omega} = \nabla \times \underline{v}$ is the vorticity. On the left hand side $L_{\parallel}$ is the length along a magnetospheric field line away from the equator that the generator mechanism acts. The left-hand side of expression (1) describes the strength of field-aligned current and the six terms on the right-hand side are driver (current-diversion) terms in the magnetosphere for that field-aligned current. The first term on the right-hand side represents pressure-gradient driving of parallel currents: for pressure driven arcs the first term on the right-hand side must dominate over all other terms on the right hand side, yielding $\nabla_{\parallel}(j_{\parallel}/B) = (2/B^3)(\nabla_{\perp} P \times \nabla_{\perp} B)$ (Grad 1964; Vasyliunas 1970). The other terms on the right-hand side of expression (1) represent flow braking, vorticity and magnetic-flux change, baroclinic flow ($\nabla T \times \nabla \rho$), and advected vorticity. In dynamical MHD simulations of field-aligned currents driven in the magnetotail, Birn et al. (1999, 2011) find that the $\nabla_{\perp} P \times \nabla_{\perp} B$ term tends to be dominant. For driving auroral arcs (with upward current coming out of the ionosphere), the vector $\nabla_{\perp} P \times \nabla_{\perp} B$ evaluated in the equatorial plane of the magnetosphere should be pointing southward. The driving of auroral arcs by pressure gradients in the Earth's plasma sheet has been suggested several times, focusing on various pressure configurations that may form in the nightside magnetosphere. In the plasma sheet typically $T_i > T_e$ and the ion pressure dominates over the electron pressure, so the focus has usually been on the ion-pressure configuration.

Three prominent applications of plasma-sheet pressure configurations driving arcs are by Stasiewicz (1985), Galperin et al. (1992), and Coroniti and Pritchett (2014). Stasiewicz (1985) hypothesized that premidnight quiescent arcs could be driven by elongated streams of lower-pressure plasma advecting from the magnetotail sunward into the duskside dipolar magnetosphere, with the auroral arc magnetically mapping to the duskward edge of the low-pressure stream where the pressure gradient $\nabla_{\perp} P$ points in the duskward direction. (Stasiewicz 1985 also discussed the possibility of electron pressure gradients caused by spatial variations of the electron temperature.) Galperin et al. (1992) (see also Galperin and Bosqued 1999) looked at an Earthward-pointing pressure gradient $\nabla_{\perp} P$ at the Earthward edge of a strong cross-tail current at a location where $|B_z|$ has a localized minimum in the magnetotail. A feedback in the cross-tail current sheet is described wherein ion stochasticity leads to a strengthened current which leads to a reduced $|B_z|$ and more stochasticity. Examining the Tsyganenko T87 magnetic-field model (Tsyganenko 1987), they argued that there is a slight misalignment of the directions of $\nabla_{\perp} P$ and $\nabla_{\perp} B$ in this $|B_z|$ minimum that make $\nabla_{\perp} P \times \nabla_{\perp} B$ nonzero. Coroniti and Pritchett (2014) analyzed a configuration wherein there is an Earthward-directed radial gradient $\nabla_r P$ duskward of midnight where the magnetic-field strength B decreases going away from midnight. They argued that if this maximum $\nabla_r P$ occurs at a location where $\nabla_y P = 0$ then field-aligned current will be maximal.

Tverskoi (cf. Antonova et al. 1998; Stepanova et al. 2003) suggested a mechanism whereby the hot-plasma pressure profile in the plasma sheet can become stratified to form multiple quiescent auroral arcs. In upward-current regions, they identified a plasma pressure feedback with the electrostatic potential (Tverskoi 1983) wherein stratified perturbation potentials in the magnetosphere grow and trap ions to produce pressure stratification; the result is a stratification of the magnetospheric plasma, the plasma pressure, field-aligned current, and magnetospheric convection. Two assumptions for this stratification instability to work are (1) that magnetospheric potential perturbations are linearly proportional to magnetospheric pressure perturbations and (2) that the magnetospheric spatial scales of the stratification perturbations are on the order of the magnetospheric ion gyroradius. The stratified plasma pressure in the magnetosphere drives stratified upward field-aligned current via the $\nabla_\perp P \times \nabla_\perp B$ current-diversion mechanism.

For pressure-driven currents, the width of the arc in the atmosphere is governed by the magnetic mapping of the scalesizes of the pressure gradient and/or magnetic-field-strength gradient from the magnetosphere to the atmosphere.

It should be noted that there are electron pressure gradients in the nightside magnetosphere that can be very sharp. The inner edge of the electron plasma sheet is often very sharp in the radial direction (Gussenhoven et al. 1981; Borovsky et al. 1998b) with the gradient scale of the hot-electron density being comparable to an ion gyroradius or an ion inertial length. The location of the electron inner edge depends on the level of magnetospheric convection (Gussenhoven et al. 1983; Elphic et al. 1999), with the edge moving deeper into the nightside dipole as global magnetospheric convection becomes stronger, e.g. during the growth phase of a substorm; as the inner edge moves deeper into the dipole its magnetic mapping to the ionosphere moves equatorward. Owing to temporal changes in the level of magnetospheric convection, multiple edges can form.

3.2 Model of Embedded Arcs

Haerendel (2007, 2008, 2009, 2010, 2011, 2012a, 2012b) has put forth an extensive model of auroral arcs "embedded" in the convection of the plasma sheet. In the model Earthward flow from the magnetotail sets up a local pressure maximum in the near-Earth magnetotail; in particular a local maximum in PV is set up, where P is the plasma particle pressure and V is the flux-tube volume. The maximum is in both the radial and azimuthal directions, with the azimuthal maximum near local midnight. To drive strong arcs, the plasma beta at the pressure maximum must be somewhat above unity. As plasma and plasma pressure build up on the nightside, the azimuthal pressure gradient pushes the plasma azimuthally around the dipolar obstacle. The magnetospheric plasma is magnetically connected to the ionosphere where ion-neutral collisions oppose the azimuthal flow in the ionosphere, leading to a twist (magnetic stress) of the plasma-sheet magnetic-field lines as the magnetospheric azimuthal flow gets ahead of the ionospheric azimuthal flow. This twist represents a magnetic stress.

At a location where the radial pressure gradient is toward the Earth (tailward of the pressure maximum) it is conjectured that a sharp "ledge" forms in the broad radial pressure gradient, the ledge being a steepened pressure gradient. This is sketched in Fig. 6. The auroral arc magnetically maps to this pressure ledge, with the width of the arc set by the width of the ledge. (Although structuring of the optical signature of the arc to smaller scales caused by Alfvén wave transits and reflections cannot be ruled out (e.g. Lysak 1985; Haerendel 1994).) Because of the sharp pressure gradients at the ledge, an intense upward field-aligned current is driven from the magnetosphere into the arc.

Because of the intense field-aligned current, a field-aligned voltage forms above the ionosphere on the arc field lines: associated with the field-aligned potential drop, the field lines

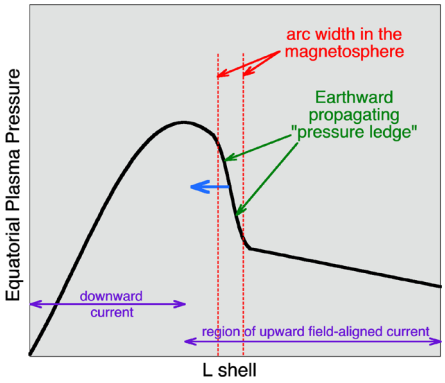

Fig. 6 A sketch of the "pressure ledge" in the plasma sheet in the embedded-arc model of quiescent auroral arcs

are no longer equipotential and there is a partial disconnection of the strong perpendicular electric field in the magnetosphere from a weaker perpendicular electric field in the ionosphere. This allows the magnetosphere's field lines to partially slip relative to the ionospheric flow. This azimuthal slippage reduces the magnetic stress on the magnetospheric field lines in the azimuthal flow in the arc. The azimuthal magnetospheric flow must do work against the opposition of the ionospheric with its ion-neutral collisions and the azimuthal magnetospheric flow must do work to power electron acceleration through the field-aligned voltage drop: the energy for this work comes from both (a) a reduction of the magnetic stress in the magnetosphere and (b) a reduction of the particle pressure in the magnetosphere (reduction of internal energy). (Earlier papers (Haerendel 2007, 2008, 2009) explicitly discussed the release of internal energy (nK_BT thermal energy) from the magnetosphere in the arc, the so-called "auroral pressure valve" (Haerendel 2000), whereas later papers (Haerendel 2010, 2011, 2012a, 2012b) discussed only the magnetic stress release supplying power to the arc.)

In the model it is hypothesized that after the local energy in the arc (and pressure ledge) is depleted, the arc will advect Earthward into the pressure gradient and utilize new magnetic-stress energy and thermal energy to keep the arc powered, tapping stress and pressure as it radially propagates through the magnetospheric plasma. The Earthward migration of the pressure ledge in the magnetosphere corresponds to an equatorward drift of the arc in the atmosphere.

The relief of magnetic stress by the decoupling of the magnetic-field connection to the ionosphere yields an azimuthal acceleration of magnetospheric plasma away from midnight at the leading edge (Earthward edge) of the arc. It is proposed that this azimuthal flow overshoots its equilibrium and begins to flow azimuthally back toward midnight, forming a return flow on the trailing edge of the arc. These forward and backward flows along the arc are consistent with $\underline{E} \times \underline{B}$ drift in a converging perpendicular electric field, i.e. a U-shaped potential around the magnetospheric portion of the arc. In the evening sector, with a vorticity $\underline{\omega} = \nabla \times \underline{v}$ that is northward in the equatorial plane, $\underline{\omega} \bullet \underline{B} > 0$ and hence the arc's vorticity layer in the magnetosphere contains a negative space charge (cf. Eq. (11) of Borovsky and Birn 2014 where the $j \bullet \underline{v}$ term inside the arc is smaller than the $\underline{\omega} \bullet \underline{B}$ term by a factor of $2B/\Delta B$ where B is the equatorial magnetic-field strength and ΔB is the diamagnetic change in the magnetic-field strength across the ledge pressure gradient at the equator).

It is stated (Haerendel 2012a) that the ultimate source of energy for the arc is the magnetospheric pressure gradient in the azimuthal direction.

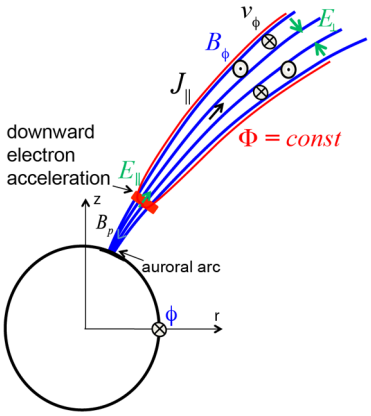

Fig. 7 Schematic of a U-shaped potential associated with the auroral acceleration region. Magnetic field lines are shown in blue, potential contours in red and electric field vectors in green. Modified after Fig. 1 of Birn et al. (2012)

3.3 Arcs Associated with Cross-Tail Current Sheets

The parallel electric field, which is the essence of electron acceleration above the atmosphere in auroral arcs, is part of a U- or S-shaped potential connected with perpendicular electric fields, as illustrated in Fig. 7. While the parallel electric field is confined to the acceleration region the perpendicular electric field maps out into the magnetosphere, although it is not fully established how far. As illustrated in Fig. 7, the converging perpendicular electric field is associated with an $\underline{E} \times \underline{B}$ drift, which would cause a shear in the magnetic field with a B_ϕ component appropriate for the upward field-aligned current in auroral arcs. Thus, the main features connecting the auroral acceleration region with the source region in the magnetosphere are the upward field-aligned current and the perpendicular electric field.

The typical scale size of quiet arcs of ~ 10 km in the ionosphere becomes close to an ion inertia length when mapped into the magnetotail. At this scale, ions are no longer frozen into the magnetic-field lines whereas the electrons are. Thus, the perpendicular electric field is associated with electron $\underline{E} \times \underline{B}$ drift, assuming that the picture is quasi-steady and the electric field maps out into the magnetosphere as a potential field. Since the ions do not (fully) participate in $\underline{E} \times \underline{B}$ drifting, the electron $\underline{E} \times \underline{B}$ drift corresponds to a Hall current, confined to a thin sheet or sheets. This has led several authors (Paschmann et al. 2002; Schindler and Birn 2002; Birn et al. 2004a, 2012; Coroniti and Pritchett 2014) to suggest a connection between auroral arcs and thin current sheets in the magnetotail. As outlined in Sect. 7.7.5 of Paschmann et al. (2002), there are several potential thin current sheet regions in the magnetotail that have locations suitable for an association with auroral arcs: the inner edge of the electron plasma sheet, the thin growth phase current sheet, the near-Earth reconnection site, the plasma sheet boundary layer, and bursty bulk flows. The association of the latter with field-aligned currents and perpendicular electric fields will be discussed in Sect. 5. Here we are particularly interested in the possible source regions of quiet arcs: the inner edge of the electron plasma sheet (cf. Sect. 3.1) and the thin growth phase current sheet.

Extreme current-sheet thinning in the inner magnetotail prior to substorm onset has been documented by observations by many authors (e.g., McPherron et al. 1987; Sergeev et al. 1993; Pulkkinen et al. 1994; Sanny et al. 1994). The main features that support theoretically the association of the thin growth-phase current sheet with the quiet arc are derived from self-consistent models or particle simulations of thin current sheets at and below the ion-inertial scales (e.g., Pritchett and Coroniti 1994; Hesse et al. 1996, 1998): (a) the fact that the current in such current sheets is carried by electron $\underline{E} \times \underline{B}$ flow, and (b) that these sheets are

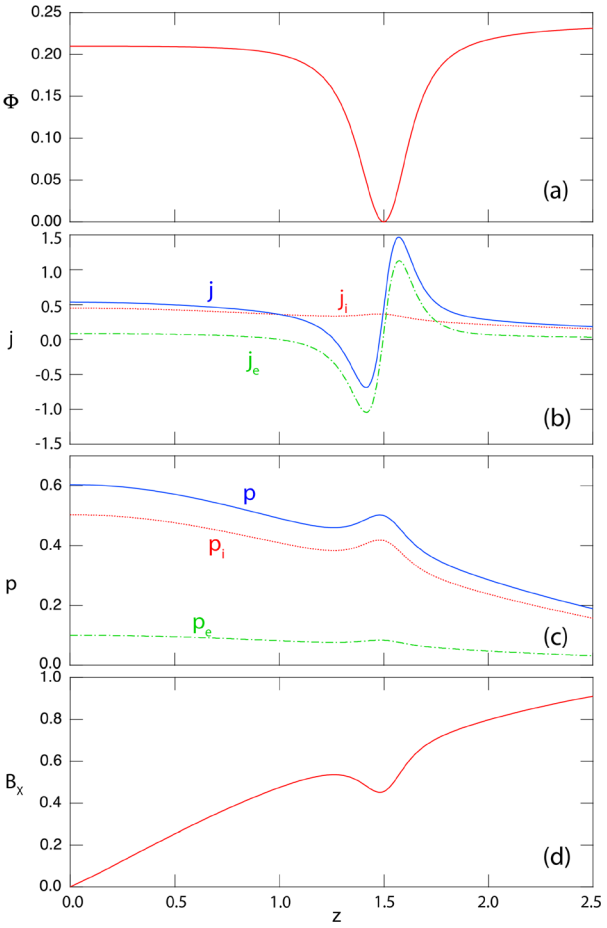

Fig. 8 Vlasov model of a thin double current sheet, suitable for the generation of converging perpendicular electric fields: (**a**) electric potential, (**b**) current density contributions, (**c**) pressure contributions, and (**d**) magnetic field component B_x as functions of z. Modified after Fig. 10 of Birn et al. (2004a)

associated with field-aligned potentials and perpendicular electric fields that could provide the connection to the auroral acceleration region. On the basis of 2-D Vlasov equilibrium theory (Schindler and Birn 2002), Birn et al. (2004a) constructed models of thin current sheets with potentials suitable for the connection to a quasi-static arc. Figure 8 shows an example with a potential that corresponds to the converging perpendicular electric field of a U-shaped auroral potential. In reproducing this figure, we noticed that the labels of p_i and p_e were misplaced in Fig. 10 of Birn et al. (2004a). It is actually common in these thin-current-sheet models that the ion pressure dominates despite the fact that the current is carried primarily by the electrons (in a frame in which the electric field vanishes outside the current sheet).

Since these models are typically two-dimensional, they do not include the field-aligned current that is a necessary ingredient for auroral arcs. However, qualitative arguments based on embedding the 2-D models in a 3-D environment indicate that the azimuthal electron flow may well be associated with field-aligned currents, as illustrated in Fig. 9. In fact, a similar field bending is part of the kinetic structure of the thin current sheet at a near-tail reconnection site and has been confirmed by the quadrupolar B_y field associated with Hall currents in particle simulations (e.g., Sonnerup 1979; Terasawa 1983; Pritchett 2001).

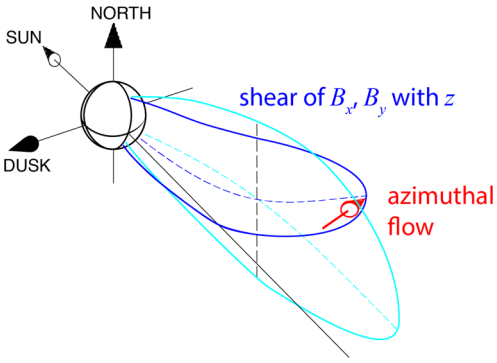

Fig. 9 Schematic of an azimuthal flow causing field-line bending and magnetic shear. Modified from part of Fig. 3.4 of Paschmann et al. (2002). The schematic was originally used to illustrate the effects of plasma flow but can also be applied to electron flow if the ions are decoupled

An auroral arc and precipitation model closely related to properties of the plasma sheet and current sheet thinning is based on so-called isotropy boundaries (Sergeev et al. 1983, 2012). The basic concept for such boundaries is the isotropy or lack of isotropy of ions and electrons observed by low orbiting spacecraft in the auroral region. The fact that the loss cone is filled is taken as an indication for effective scattering of particles into the loss cone and has been associated with chaotic particle motion in the plasma sheet (Buechner and Zelenyi 1986, 1989; Sergeev et al. 1990). (Note that in the magnetotail plasma sheet there is an absence of waves that would pitch angle scatter ions (e.g. Usanova et al. 2012) and, unless reconnection is ongoing, an absence of waves that would pitch-angle scatter electrons Zhang et al. 1999.) The relevant parameter for chaotic motion is the ratio $\kappa^2 = R_c/r_g$, where R_c is the radius of curvature of the magnetic field in the center of the tail current sheet and r_g is the (90°-pitch-angle) gyroradius in the center field. When this ratio κ^2 is sufficiently small particle motion is strongly nonadiabatic and scattering can easily fill a loss cone caused by auroral precipitation. It is obvious that more energetic particles with larger gyroradii are more easily nonadiabatic, and ions are less adiabatic than electrons. The dependence on the radius of curvature implies that nonadiabaticity increases for thinner current sheets.

The radius-of-curvature scattering mechanism has been employed to categorize types of precipitation based on low orbiting spacecraft (e.g., Newell et al. 1996b; Wing et al. 2005), to identify ground based precipitation boundaries (Donovan et al. 2003), and to improve mapping between the plasma sheet and the ionosphere (Shevchenko et al. 2010; Kubyshkina et al. 2011). Using ground, low altitude, and plasma sheet THEMIS observations, Sergeev et al. (2012) used an adaptive magnetic-field model to identify the magnetospheric location of the pre-breakup (growth-phase) arc. Figure 10 presents the comparison of optical and low orbiting energetic particle data for parallel and perpendicular energy fluxes, illustrating the isotropy boundaries and the good agreement between the isotropy boundary of the energetic electrons with the optical arc location. Comparison with the adaptive magnetic-field model implies an arc location at the most-earthward edge of a thin cross-tail current sheet.

In separate computational studies Yang et al. (2013) and Hsieh and Otto (2014) examined the formation of a very thin cross-tail current sheet based on adiabatic convection from the midnight tail region to the dayside and its mapping into the auroral ionosphere. In both studies, the imposed convection generated a strong magnetic-flux depletion in the midnight sector causing an equatorward expansion of all auroral signatures/proxies. Figure 11 (top) from Hsieh and Otto (2014) presents the field-aligned current pattern mapped into the ionosphere at the start of the simulation, corresponding to the currents from the Tsyganenko model used to initialize the simulation. The bottom left of Fig. 11 shows the field-aligned currents 45 minutes into the simulation with the maximum current density almost an order

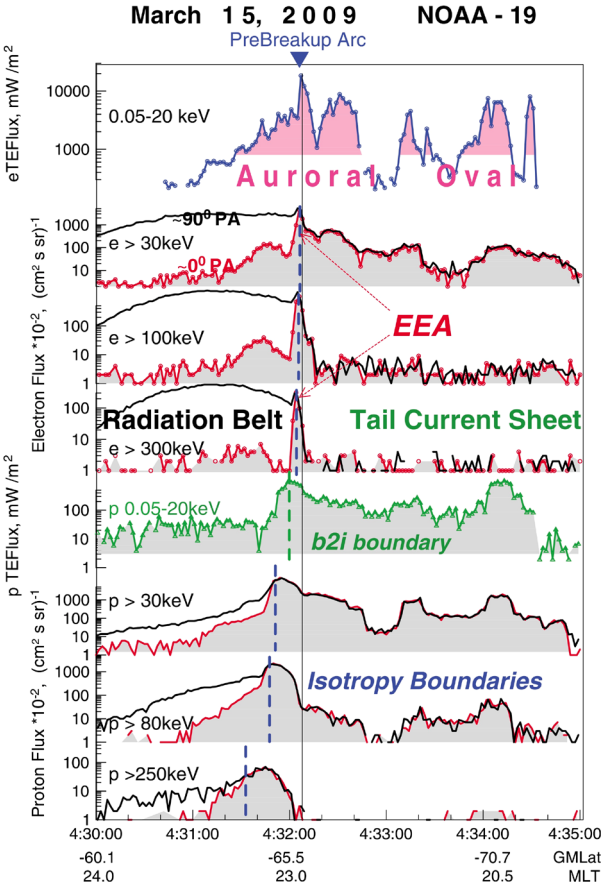

Fig. 10 Comparison of auroral energy flux and parallel (red) and perpendicular (black) particle flux for different electron and ion energy ranges from Sergeev et al. (2012)

of magnitude higher, much narrower, and by about 2 degrees further equatorward. Using a value of $\kappa = 8$ the yellow and black solid lines show the mapping of the 100-keV electron and 30-keV ion isotropy boundaries with the electron isotropy boundary at the equatorward edge of the thin region 1 field-aligned current. The bottom right of Fig. 11 shows the equatorial magnetic-field strength mapped as a reference to the two isotropy boundaries. While Yang et al. (2013) used the modified Rice Convection Model, Hsieh and Otto (2014) used a mesoscale MHD simulation. However, results are quantitatively very similar regarding field-aligned current evolution, motion, and isotropy boundary as a proxy for precipitation energy. Note, that the mechanism for the field aligned current evolution is the same as illustrated in Fig. 9.

3.4 Stationary Alfvén-Wave Arc Picture

Auroral arcs are a signature of magnetosphere-ionosphere coupling via fields and particles. For quasi-static arcs, the relevant timescales are from minutes to tens of minutes. This is in the domain of Alfvén waves, which are defined as having a characteristic frequency ω much less than the relevant ion cyclotron frequencies. In principle, ω can extend to zero, meaning quasi-static fields can be treated as Alfvén waves after all transients have died out. However the question then arises as to why a wave treatment is necessary. The answer is

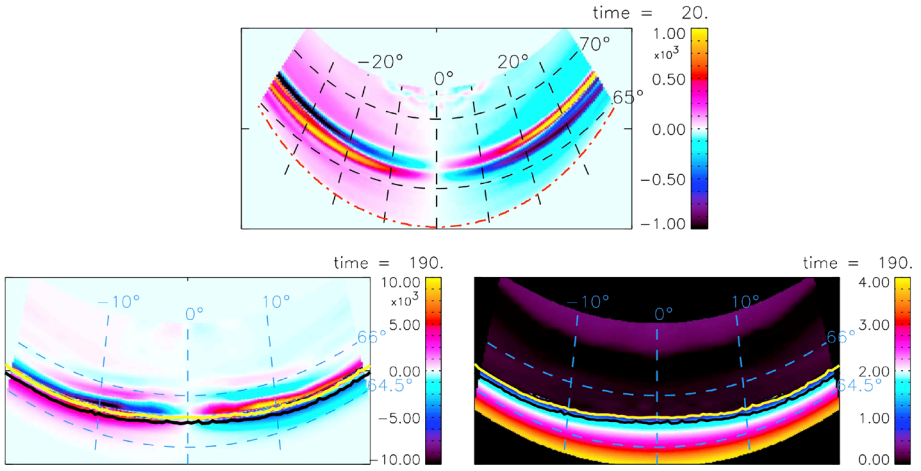

Fig. 11 Mapping of field-aligned currents into the ionosphere at the beginning of the simulation (top) and after 45 minutes (bottom left). Yellow and black traces show the isotropy boundaries for 100 keV electron s and 30 keV ions. The lower left plot represents the equatorial tail magnetic field magnitude mapped into the ionosphere (1 unit corresponding to 20 nT). From Hsieh and Otto (2014)

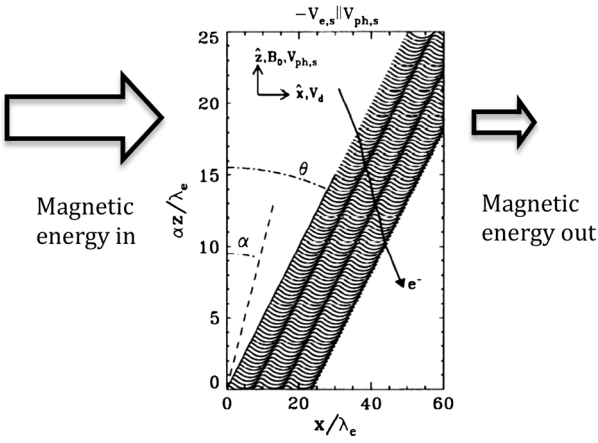

Fig. 12 In a non-drifting reference frame (e.g. channels of enhanced conductivity in the ionosphere) the current sheet coupling the magnetosphere and ionosphere can be susceptible to spatial structuring of electron density (plotted here) and field-aligned energy powered by advection of magnetic energy. After Knudsen (1996)

that various wave-like behaviors arise in quasi-static situations where sources of perturbed fields or currents move relative to the background plasma (Jupiter's moon Io is an example), or equivalently when plasma convects past stationary sources.

The term "stationary Alfvén wave" was used by Maltsev et al. (1977) and Mallinckrodt and Carlson (1978), who considered plasma convection across a localized ionospheric conductivity enhancement and showed that the resulting field-aligned currents propagate upward as a localized shear Alfvén wave with a wavefront that is inclined with respect to the magnetic field by the small Mach angle $\alpha = \mathrm{Arctan}(v_{\mathrm{drift}}/v_{\mathrm{A}})$. A stationary Alfvén wave is depicted in Fig. 12. (Such structures can also be described as "Alfvén wings" (e.g. Drell et al. 1965).) This wave can reflect in the conjugate ionosphere, however the net effect of convection and the relatively slow Alfvén wave speed (relative to c) is to displace the return wave in latitude relative to its source (Gurnett and Goertz 1981). Multiple bounces can occur, and are put forward by Maltsev et al. (1977) and Mallinckrodt and Carlson (1978) as a possible

explanation of multiple auroral arcs. Once a quasi-static steady state is reached, the Alfvénic character of the structures is maintained by polarization currents resulting from plasma convection across stationary field structures, which are then closed via field-aligned currents.

These original stationary-Alfvén-wave models do not provide a self-consistent mechanism for the creation of parallel electric fields and particle acceleration. Furthermore, auroral arcs and multiple arc systems are observed to form on timescales of seconds, much faster than the inter-hemispheric Alfvén-wave bounce period of many minutes. Lysak (1991) explored wave reflections within the topside ionospheric Alfvén resonator, which has a fundamental resonant frequency of the order of 1 Hz, as a means of reducing the growth time and creating small-scale structure through multiple interfering reflections. Lysak and Song (2002) argued that the energy for such structures derives from a reduction of Joule heating associated with the large-scale convection electric field; in the case of quiet-time background convection this is insufficient to power auroral arcs.

Knudsen (1996) developed a model of stationary inertial Alfvén (SIA) waves based on a two-fluid (ion and electron) model that included several new effects including (a) finite electron inertia allowing finite $E_\parallel$, (b) a source of $E_\parallel$ of the order of $E_c \delta B / B_0$ arising through the interaction between the perturbed magnetic field δB and the convection electric field E_c (Seyler 1990), and (c) self-consistent inclusion of advection and associated nonlinearities. Solutions were then sought in the form of stationary wavefronts resulting (after all transients have died away) from propagation along B at speed of the order of (but not necessarily equal to) the Alfvén speed, with a superimposed uniform background convection electric field E_y which is normal to all density and field variations. In other words, the model allows for two-dimensional arc-like structures having a uniform background convection flow in the cross-arc direction (x) and no variation in y. Finnegan et al. (2008) added the effects of finite electron temperature and collisions.

An important additional element of the Knudsen (1996) model is an imposed, large-scale background field-aligned currents sheet, the source of which is unspecified. Within such a sheet, the model admits solutions of in the form of nonlinear spatially-periodic oscillations in density, field-aligned electron energy, field-aligned currents, and electric field (perpendicular and parallel to B). The allowed wavelengths of these structures across B are several to tens of electron inertial lengths λ_e, more than an order of magnitude of larger than the $\lambda_\perp$ values associated with electron acceleration by time-varying inertial Alfvén waves. For example, taking nominal auroral acceleration region densities in the range 10–1000 cm^{-3} at an altitude of 4,000 km gives λ_e mapped to the ionosphere of 0.8–8 km, leading to SIA wavelengths across B of several to tens of km. Unlike the case of time-varying inertial Alfvén waves, electron acceleration by SIA waves is not limited by the Alfvén speed and electrons can reach many times V_A, corresponding to energies much greater than 1 keV. However, the model of Knudsen (1996) cannot produce such energies within the observed field-aligned extent of the auroral acceleration region ($\sim$ 10,000 km). Furthermore, that model does not account for several potentially important effects such as an ionospheric boundary and variations in the background plasma (e.g. density and magnetic field). For this reason, the model does not make predictions that are specific to the terrestrial M-I coupling region, for example the altitude of the electron acceleration region. Addressing these issues will require a proper numerical simulation as opposed to the analytical models used by Knudsen (1996) and Finnegan et al. (2008).

SIA waves can be thought of as the electromagnetic analog of perturbations in a fast-flowing river. They are not standing waves in the sense that there is no sinusoidal variation in time. Rather, they are stationary spatial structures resulting from the flowing fluid. The assumed background field-aligned currents, in addition to being necessary to give rise to

the spatially periodic solutions described above, also provides a source of energy, namely advection of magnetic energy, that is comparable to observed values (Knudsen et al. 2011). The concept of magnetic energy as a source of energy for auroral arcs was proposed by Haerendel et al. (1993) for the case of time-varying (shrinking) current sheets.

3.5 Feedback-Instability-Driven Arcs

The feedback instability in magnetosphere-ionosphere (M-I) coupling was proposed as a possible formation mechanism of quiet auroral arcs (Atkinson 1970; Sato and Holzer 1973; Sato 1978): the feedback is between field-aligned currents and the conductivity variations produced by those currents. The simplest M-I coupling model for the feedback instability is described by the magnetohydrodynamic equations for the magnetosphere and the height-integrated two-fluid equations for the ionosphere, where the spatiotemporal scales are assumed to be much longer than the ion gyroradius and gyroperiod. The ionospheric equations consist of the continuity of particles and currents, along with charge neutrality. In the steady state with constant ionospheric density, the latter is simply given by the divergence free condition of the electric current, suggesting a current circuit in the M-I coupling.

To explain the physical mechanism of the feedback instability, let us suppose first that a large-scale $\underline{E} \times \underline{B}$ convection flow is set up in the equilibrium state of the magnetosphere, and the perpendicular electric field $\underline{E}$ is mapped onto the ionosphere where Pedersen and Hall currents are driven by the electric field. The Joule dissipation in the ionosphere is balanced with the input Poynting flux from the magnetosphere. If a density perturbation arises in the ionosphere, it causes a polarization electric field $\underline{E}$ as well as a perturbation of the ionospheric and the field-aligned current $j_\parallel$. Continuity of $\underline{E}$ and $j_\parallel$ between the ionosphere and the magnetosphere demands propagation of electromagnetic perturbations in the magnetosphere, that is, shear Alfvén waves.

Consider the same process occurring in both hemispheres, or suppose a symmetry or anti-symmetry condition at the magnetic equator. This scenario is supported by the conjugacy of auroral appearance on closed field lines. Then, there exist upward and downward propagating waves carrying $j_\parallel$. If the upward and downward components of $j_\parallel$, respectively, coincide with the ionospheric density increase and depletion, the perturbation may be enhanced. This is because the electron precipitation increases the plasma density (or conductivity) in the ionosphere, and vice-versa. In contrast, if the electron precipitation carrying the upward $j_\parallel$ is in phase with the density depletion, the perturbation may be damped. This situation is possible only when one takes into account the time-evolution of the ionospheric density. Then, the perturbations of density, $\underline{E}$, and $j_\parallel$ satisfying the unstable phase relation can grow exponentially in time in the linear regime, leading to the feedback instability in the M-I coupling.

The free energy for the feedback instability comes from reduction of the ionospheric Joule heating (Lysak and Song 2002). As discussed above, the background convection electric field leads to steady Joule heating in the equilibrium state, if the ionospheric density is constant in time. When the ionospheric density perturbation arises, a local reduction of the Joule heating releases energy to the Alfvén waves reflected at the ionosphere, which can be characterized as an over-reflection of the Alfvén waves. The same conclusion can be derived from the energy balance equation for the reduced MHD and the ionospheric equations, where the input Poynting flux provided by the equilibrium-scale electric field and the field-aligned current (inducing the magnetic field) turns out to be the energy source.

The feedback instability has been shown to be excited under realistic parameters when the convection electric field exceeds a critical value related to the stabilization effects of recombination loss or diffusion in the ionosphere. The linear theory predicts the most unstable

wave length of fluctuations once the ionospheric and magnetospheric parameters are given. This provides an important implication to the theory of auroral arcs. The feedback instability potentially explains typical spatiotemporal scales of auroral arcs, which are selected by the M-I coupling system itself (rather than external conditions) if the equilibrium state with characteristic parameters are given.

The most unstable fluctuation propagates in the direction of the ionospheric current with a phase speed characterized by the Pedersen and the Hall mobility (Watanabe 2010), while the real frequency is roughly scaled by that of the field line resonance. If the Alfvén velocity is non-uniform, and has a sharp gradient along the field line, a partial reflection of the Alfvén waves enables stronger feedback M-I coupling with higher frequencies and growth rate than those of the entire field line resonance (Lysak 1991). The feedback instability is further enhanced when one introduces the ionization effect of neutrals due to precipitating electrons (Sato 1978).

Morphological features of the feedback instability are described below. Local density enhancements and depletions are generated by the feedback instability in the ionosphere. A pair of upward and downward field aligned current, that is, a local current circuit, is also spontaneously formed, where the upward current $j_{\parallel}$ carried by precipitating electrons generates auroral arcs with density increase. Simultaneously, the electric field perturbation drives the local $\underline{E} \times \underline{B}$ flow with a perpendicular velocity shear not only in the ionosphere but also in the magnetosphere. The sheared flow adjacent to auroral structures may induce a secondary (nonlinear) instability if the primary feedback instability can grow to a large amplitude. Recent nonlinear simulation of the M-I feedback coupling reveals the secondary excitation of the Kelvin-Helmholtz type instability, which leads to roll-up of auroral vortex structures (Watanabe 2010; Watanabe et al. 2016). While direct observational evidence for the feedback instability is rare, recent work analyzing sounding rocket data has shown characteristic consistent with the feedback instability (Cohen et al. 2013).

The above discussions are limited to the simplest model of M-I coupling with uniform magnetic field and the reduced MHD model for the magnetosphere. A variety of extensions of the feedback instability has also been discussed in the literatures, such as the global distribution of arc structures (Miura and Sato 1980; Watanabe and Sato 1988; Watanabe et al. 1993, 1994), introduction of the two-fluid effects (Streltsov and Lotko 2003, 2004, 2008), application to the dipole geometry (Lu et al. 2007, 2008; Hiraki and Watanabe 2011, 2012), fine structure formation (Jia and Streltsov 2014; Watanabe et al. 2016), and gyrokinetic model for the magnetosphere (Watanabe 2014). Sydorenko and Rankin (2017) have argued that height variation of the ion-neutral collision frequency in the ionosphere inhibits the feedback instability; the generality of this conclusion is disputed by Watanabe and Maeyama (2018) and Streltsov and Mishin (2018). Overall, further elaboration is necessary for a complete understanding of ionospheric feedback in the M-I coupled system, including parallel electric field generation and auroral particle acceleration, coupling with pressure perturbations, nonlinear dynamics and turbulence transition, and a realistic three-dimensional geometry that can resolve auroral fine structures.

4 Considerations for Arc and Oval Current System Near the Harang Region

As detailed in Sect. 1.4 of Paschmann et al. (2002), observations near the low-altitude end of the auroral-current circuit suggest that one-dimensional planar symmetry, which is often assumed for quiet auroral arcs, may not hold at specific locations and times, notably in the

Harang region during the substorm growth phase. Likewise, the auroral oval may not be azimuthally symmetric. Here we briefly address the effects of the modified arc and oval symmetry on the auroral current circuit and its magnetospheric generator.

Two basic configurations of the auroral current circuit were proposed by Boström (1964), remarkably enough, at a time when the existence of field-aligned currents had not been confirmed yet (cf. Fig. 4).

Boström's "Type 1" auroral current circuit relies on a pair of filamentary field-aligned currents that are connected to each other by a Cowling channel in the ionosphere driven by a primary electric field in the approximately east-west direction. The Type-1 auroral circuit is powered by a magnetospheric generator dominated by an electric field and current in the azimuthal direction. The ionospheric electrojet includes a Pedersen component that is associated with the primary east-west electric field and a Hall component that is associated with a secondary north-south polarization electric field. Subsequently, the Type-1 circuit was found to be realized on a large scale by the substorm current wedge (McPherron et al. 1973; Birn and Hesse 1991; Scholer and Otto 1991; Keiling et al. 2009) and on smaller scales by the current "wedgelets" (Rostoker 1998) related to high speed plasma flows in the magnetotail (Sergeev et al. 1996, 2000; Birn et al. 2004b; Liu et al. 2013).

Boström's "Type 2" auroral current circuit relies on a pair of sheet field-aligned currents connected to each other by a north-south Pedersen current. The Type 2 circuit is powered by a magnetospheric generator dominated by an electric field and current in the radial direction. The east-west Hall electrojet driven by the primary north-south ionospheric electric field is divergence free. Type-2 circuits are realized by the auroral arc current system (e.g. Elphic et al. 1998) and on auroral-oval spatial scales by the Region 1/Region 2 currents (Iijima and Potemra 1978). As such, Type 2 geometries underlie the one-dimensional aurora-arc and oval models mentioned above.

Since aurora can be quite complex, in particular during substorms, Type-1 and Type-2 configurations can co-exist, possibly embedded in each other. An example is auroral arcs embedded in the westward travelling surge, related to the upward field-aligned current filament of the substorm current wedge (e.g. Marklund et al. 2012). With due care to real-world complexity, the Type-2 configuration can be regarded as typical for the current system of the quiet arc and oval, while the Type-1 configuration appears to describe the auroral current circuit under more dynamic conditions.

The events investigated by Marghitu et al. (2004, 2009, 2011) at the low-altitude end of the auroral current circuit show a different mix of Type-1 and Type-2 circuits, in some sense a hybrid between the two with field-aligned current sheet geometry specific to Type 2 and field-aligned current-electrojet coupling specific to Type 1. Statistical evidence gathered by Jiang et al. (2015) appears to confirm that field-aligned current-electrojet coupling may indeed make a significant contribution to the ionospheric field-aligned current closure of the growth phase auroral arc prior to break up at substorm onset. Other studies (e.g. Zou et al. 2009) indicate that such arcs are often located in the Harang region.

The effect of the topology of the ionospheric field-aligned-current closure currents on the magnetospheric generator end of the auroral current circuit was addressed by Marghitu et al. (2009). In the Harang region poleward of the convection reversal boundary the coupling of the upward field-aligned current to the westward electrojet suggests that there is azimuthal field-aligned current closure in the magnetosphere with a current opposite to the cross-tail current and contributing to the current disruption at the substorm onset. The magnetospheric current of the westward-electrojet loop is also opposite to the dawn-to-dusk magnetospheric electric field, denoting a magnetospheric generator that drives the ionospheric dissipation in the upward current region (Fig. 4). Depending on how much of the field-aligned current

closure is achieved by the Pedersen and Hall component of the ionospheric current, energy dissipation can be dominated by Joule heating when Pedersen closure prevails or by accelerated particle heating when Hall closure prevails.

Likewise, equatorward of the convection reversal boundary the coupling of the downward field-aligned current to the eastward electrojet indicates that the magnetospheric segment of this current loop has the same sense as the ring current and may contribute to the evening-sector asymmetry of the ring current as inferred from ground magnetic data (e.g. Newell and Gjerloev 2012) and energetic-neutral-atom imaging (e.g. Brandt et al. 2018). Future work is needed to investigate the relationship between the time variation of the ring current asymmetry and the substorm cycle.

5 What Global and Magnetotail Computer Simulations Say About Driving Auroral Arcs

At first, the topic of this section appears to be an oxymoron. In Sect. 3.3 we have argued that the arc size investigated in this review paper involves scales short enough for a breakdown of the frozen-in condition when mapped to the presumed magnetotail source region, implying a separation of ion and electron motion. However, the two important elements in arc generation are the establishment of field-aligned currents that connect the source region with the arc dissipation region and the generation of perpendicular electric fields that allow the closure through the parallel potentials essential for the auroral acceleration region. These elements are essential ingredients not only on electron scales but also on larger ion or fluid scales treated in MHD simulations, such that conclusions from the MHD simulations may also apply to shorter scale mechanisms. Arc models of the stationary Alfvén waves and the feedback instability are the examples that relate the MHD dynamics to auroral fine structuring.

In this section we address mechanisms of field-aligned current generation on the basis of local magnetotail simulations, which are confined to the magnetotail source region and involve a detailed study of source mechanisms, and through global simulations, which also include a self-consistent coupling with the inner magnetosphere and ionosphere.

5.1 Local Magnetotail Simulations

The details described in this section are largely based on a simulation (Birn et al. 2011) that models the onset and dynamic evolution of magnetic reconnection in the magnetotail together with the generation of flow bursts and dipolarization fronts, limited to a region tailward of about $x = -7.5\ R_E$. This and similar simulations have been used to investigate field-aligned current generation applicable to the substorm current wedge (SCW) as a whole (Birn and Hesse 1991; Scholer and Otto 1991; Birn et al. 2004b; Keiling et al. 2009), as well as to individual flow bursts, which may contribute to the SCW as "wedgelets" (Liu et al. 2013; Birn and Hesse 2013, 2014).

The main mechanism is illustrated in Fig. 13, modified after Birn et al. (2004b). The vorticity associated with a flow from the magnetotail, its braking and diversion, causes buildup of magnetic shear or twist, that is, field-aligned current. Figure 13 illustrates only the twist on the western or duskward edge, which causes the buildup of outward current. A similar but opposite twist is generated at the downward edge, causing earthward field-aligned current, thus completing the standard current system of the substorm current wedge. However, from

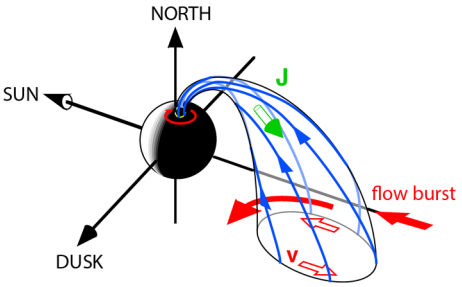

Fig. 13 Mechanism of field-aligned current generation or intensification by flow vorticity. Modified after Birn et al. (2004b)

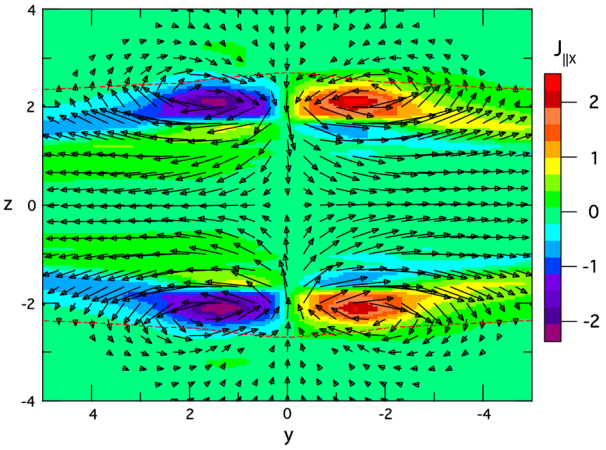

Fig. 14 Field-aligned currents and $\underline{E} \times \underline{B}$ flow vectors near the inner boundary of an MHD simulation of tail reconnection, dipolarization, and flow bursts (Birn et al. 2011). Color indicates the x component of $\underline{J}_{\|}$ with red indicating earthward currents and blue tailward currents

an auroral-arc point of view the outward current, corresponding to precipitating electrons, is of primary interest.

It should be noted that this fluid picture can also be applied on smaller scales to the electron fluid, when ions are no longer frozen in the fluid but electrons are. In that case, that difference between electron and ion flow represents a Hall current, such that Hall current layers may be considered as possible source regions for field-aligned currents on sub-ion scales (e.g., Birn et al. 2012; Coroniti and Pritchett 2014) as discussed in Sect. 3.1.

The buildup of field-aligned currents by flow shear includes self-consistently another crucial element for auroral arcs. The flow, which on small scales is carried only by electrons, is associated with a converging perpendicular electric field, which is necessary for the closure through parallel potentials. (Because there is a nonzero vorticity in the perpendicular-to-$\underline{B}$ flow $\nabla_\perp \times \underline{v}_\perp \neq 0$ with $\underline{v}_\perp = -\underline{E}_\perp \times \underline{B}/B^2$, vector identities yield $(\nabla_\perp \bullet \underline{E}_\perp)\underline{B}/B^2 \neq 0$.) This flow and perpendicular electric field exist not only near the equatorial plane, where the driver might be, but extends to higher latitudes. This is illustrated by Fig. 14, which shows the field-aligned current near the inner Earthward boundary of the magnetotail simulation of Birn et al. (2011) together with $\underline{E} \times \underline{B}$ velocity vectors in the y, z plane.

So far, we have discussed the flow pattern as a mechanism of build-up of field-aligned currents. In principle, if ionospheric dissipation and magnetospheric relaxation were neglected, the field-aligned currents would keep flowing without further need of a flow driver. In that case, it might not be possible to infer the field-aligned currents from a flow pattern and it is common to deduce them from force balance and current continuity via the Vasyli-

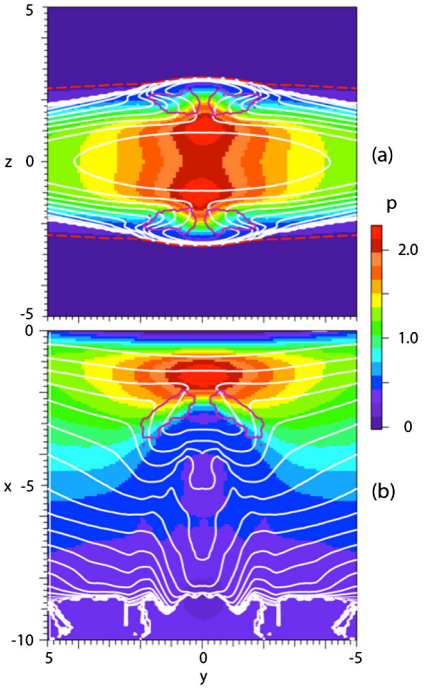

Fig. 15 (**a**) Plasma pressure (color) and contours of constant flux tube volume V (white), defined by (2), at $x = -1$, (**b**) same at $z = 0$, evaluated at $t = 130$. Purple contours indicate enhanced field-aligned currents evaluated from Vasyliunas' equation (2). The red dashed line (top) represents the open/closed boundary. After Birn and Hesse (2013)

unas formula (cf. expression (1)), here generalized to include the inertia term,

$$j_{\parallel} = -(\underline{\boldsymbol{B}}/B) \bullet (\nabla P + \rho dv/dt) \times \nabla V, \tag{2}$$

where V is the volume of a magnetic flux tube of unit flux, defined by

$$V = \int B^{-1} ds, \tag{3}$$

with s being the distance along the flux-tube axis. We note that expression (2) does not describe pressure gradients or inertia as a "driver" in a causal sense but merely an association between the different terms. An evaluation of Eq. (2) on the basis of the Birn et al. (2011) simulation showed that the dominant "driver" of the field-aligned currents is the pressure gradient term, even under dynamic conditions. This is demonstrated by Fig. 15, taken from Birn and Hesse (2013).

5.2 Global MHD Simulations

The connection between magnetotail dynamics and auroral features has been investigated in a number of global MHD simulations, modeling the interaction of the magnetosphere with the driving solar wind as well as the dissipation and current closure in the ionosphere. In the global simulations nightside field-aligned currents resembling auroral currents are identified, the currents are traced and their origins established, and their roles in the global magnetosphere are investigated. Of course global MHD simulations lack the kinetic physics and field-aligned potential drops to fully simulate auroral arcs.

Ge et al. (2011) simulated an event observed by THEMIS and were able to reproduce several of the observed features, such as auroral breakup, poleward expansion and the westward traveling surge. The breakup in particular was found to be related to a flow burst in the tail, producing strong flow shear at the edges of the flow channel, as illustrated in Fig. 13. Raeder et al. (2012) demonstrated a connection between ballooning instability in the tail and auroral beads, which are frequently observed in preexisting arcs prior to substorm onset (e.g., Liang et al. 2008; Henderson 2009). With global simulations Wiltberger et al. (2015) investigated flow bursts from reconnection in a global MHD simulation, confirming the details discussed in Sect. 5.1: an enhancement in B_Z and a decrease in density preceding a peak in the flow velocity, and a reduction of field line entropy. They also showed that the fast flow perpendicular to the magnetic field at the equator was turned into field-aligned flow off the equator.

The magnetotail connection with aurora was investigated in a series of global simulation studies of substorms done by Tanaka's group (Tanaka et al. 2010, 2017; Tanaka 2015; Ebihara and Tanaka 2015a,b, 2016), who did not aim at modeling particular substorms but rather investigated the physical mechanisms governing the interaction of magnetospheric and ionospheric processes. The initial state of the magnetosphere-ionosphere system was set up for stationary convection under northward IMF (Tanaka 2007). This was followed by a southward turning of the imposed IMF. Upward field-aligned currents, used as proxy of electron precipitation, were interpreted to be related to the possible quiet arc formation in the substorm growth phase, the onset arc brightening, and into the development and evolution of the westward traveling surge, observed, e.g., by Kadokura et al. (2002).

Ebihara and Tanaka (2016) identified field-aligned current systems, which they related to N-S arcs and the quiet preonset arc. The quiescent-arc intensification in the substorm growth phase was found to be related to an off-equatorial concentration of a high-pressure region under enhanced convection, occurring when the IMF in the global simulation was changed from weakly northward to strongly southward. This simulation of Tanaka et al. (2017) showed that the current attributed to quiet growth-phase arcs was found not to come from the equatorial region of the plasma sheet, but rather from the flow shear at the plasma sheet-lobe boundary, which is a part of the magnetospheric convection in the growth phase (cf. Sect. 5.1). The growth-phase arc was magnetically connected to the equatorial mid-tail plasma sheet; however, current lines do not follow magnetic-field lines and the current of the arc mapped to the outer edge of the plasma sheet. This current system, belonging to the Region 1 system, is shown in Fig. 16. An ultimate generator location for the current was attributed to the mantle region (Tanaka 1995) and it was noted that the current did not pass through the equatorial region of the plasma sheet.

In contrast to the setup of the quiet arc system, Ebihara and Tanaka (2015a) concluded that the initial brightening of the arc at substorm onset was generated by a near-Earth dynamo. Similar to the picture drawn from the local simulations, this dynamo was found to be related to high-speed earthward flow in the plasma sheet, resulting from the release of the magnetic tension due to reconnection at a near-Earth neutral line (Tanaka et al. 2017). The dynamo was driven by the squeezing of plasma along the field lines by the field-aligned Earthward flow driven by a field-aligned pressure gradient from the high-pressure plasma in the magnetotail plasma sheet in front of the Earthward flow burst in the equatorial plane. The upward field-aligned current attributed to the substorm-onset brightening in the simulation was located equatorward of the quiet auroral arc at a location consistent with observations by Akasofu (1964).

Similar pressure enhancement in the Earthward portion of a collapsing magnetic flux tube was also found in magnetotail simulations (Birn et al. 2004b). The pressure enhancement is associated with a local depression of the magnetic-field strength, corresponding to

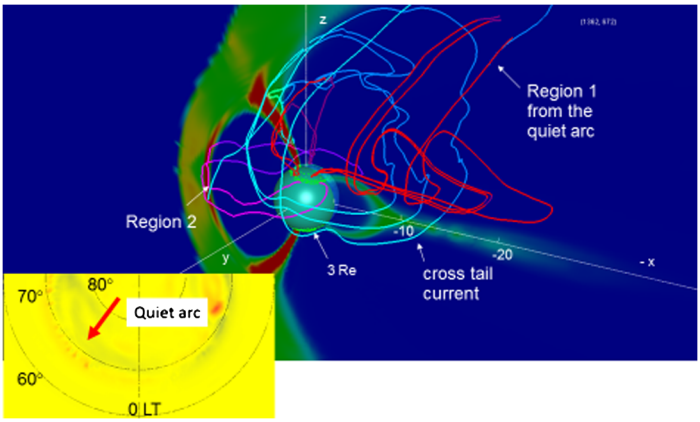

Fig. 16 The current system of the quiet arcs (red). The color shading stands for thermal pressure in the noon-midnight meridian. The left-bottom insert shows ionospheric distribution of the field-aligned current in the growth phase

a current perturbation (counterclockwise in the northern hemisphere; Birn et al. 2004a; Ebihara and Tanaka 2015a) that reverses the cross tail current below the field depression but enhances it above. The downward current below together with the duskward electric field in the collapsing flux tube constitute the dynamo interpreted by Ebihara and Tanaka (2015a) and Tanaka et al. (2017) as the source of the arc brightening.

Birn et al. (2004a) also noted that the perturbed current system is equivalent to the Hall currents associated with the perpendicular electric fields above a V-shaped auroral potential, if driven by electron flows at scales below the characteristic ion scales, as discussed in Sect. 3.1. However, it has not been shown yet that these current perturbations can be setup also at sub ion scales.

The Tanaka et al. (2017) simulation reproduced the two-step onset (initial brightening and the westward traveling surge) observed in a substorm by Kadokura et al. (2002). However, the MHD simulation cannot reproduce the actual enhancement of the auroral luminosity nor the electron precipitation, and because the mesh size in the ionosphere was as large as 100 km, the thin arc structure of the quiet arc could not be resolved. However, the upward field-aligned current, used as proxy of electron precipitation and auroral arc brightening, may be a seed of the thin auroral form generated by the feedback instability (Watanabe 2014).

It is important to note that the investigation of dynamo action, emphasized by Tanaka, is different from, but not necessarily contrary to, the consideration of flow shear and current diversion stressed particularly in Sect. 5.1. It concerns the conversion of energy (primarily from thermal transport) into magnetic energy and Poynting flux, which is the ultimate energy driver of auroral arcs. This energy conversion typically takes place closer to Earth and off the equatorial plane (e.g. Hamrin et al. 2009, 2011; Marghitu et al. 2010) in contrast to the flow shear that might be driven at or near the equatorial plane.

6 Summary and Outstanding Issues

The physical processes that act in the magnetosphere to drive quiescent auroral arcs are not known; several candidate mechanisms that have been put forth in the literature were

reviewed in Sect. 2 for high-latitude quiescent arcs and in Sect. 3 for low-latitude quiescent arcs. Predictions for the various driver mechanisms are collected in Table 1. Strengths, weaknesses, and accuracies of the various models can be judged via future evaluations of the predictions in Table 1. Presently, the form of the energy that is extracted from the magnetosphere to power the arcs is not known, and so the impact of auroral arcs on the dynamics of the magnetospheric system is not known.

Much of the uncertainty about the magnetospheric mechanisms that drive low-latitude quiescent arcs comes from an uncertainty about the magnetic connection of visible atmospheric arcs out into the nightside magnetosphere: there are on one hand arc observations and low-altitude measurements of auroral arcs and on the other hand data sets of equatorial magnetospheric measurements, but unambiguously connecting them together has not been possible. This will remain true in the near future making evaluations of Table 1 uncertain.

Spacecraft mission designs have been suggested to connect equatorial magnetospheric measurements to visible auroral forms using energetic electron beams fired from magnetospheric spacecraft into the atmospheric loss cone (Borovsky et al. 1998c; Borovsky 2002; NASA 2003; National Research Council 2012; Delzanno et al. 2016; Borovsky and Delzanno 2019), but such missions have yet to fly.

In advancing the theoretical understanding of auroral-arc driving by the magnetosphere, large-scale kinetic plasma simulations are needed. Specifically, kinetic simulations that encompass the entire auroral-arc region from the equatorial magnetosphere to the resistive ionosphere, that included nonzero-beta plasma dynamics, Alfvén-wave transmission, charge-separation electric fields, collisionless Hall currents, ionospheric Pedersen and Hall currents, ionospheric dissipation, and ionospheric ion and electron outflows would be helpful tools.

Another potential tool for discerning the driver mechanisms of arcs is machine learning and data analytics (Bobra and Ilonidis 2016; Camporeale et al. 2018; McGranaghan et al. 2018), statistically connecting up auroral observations and magnetospheric spacecraft measurements.

Acknowledgements The authors wish to thank Johan De Keyser, Mike Henderson, Michael Hesse, Joseph Lemaire, Bill Lotko, Romain Maggiolo, Noora Partamies, Michael Roth, and Michelle Thomsen for helpful conversations. JEB was supported by the NASA Heliophysics LWS TRT program via grants NNX16AB75G and NNX14AN90G, by the NSF GEM Program via award AGS-1502947, by the NASA Heliophysics Guest Investigator Program via grants NNX17AB71G, by the NSF SHINE program via award AGS-1723416. JB acknowledges support by NASA grants 80NSSC18K0834 and 80NSSC18K1452 and NSF grant 1602655. MME acknowledges support from the Romanian Ministry of Research (PCCDI Grant VESS), the Romanian Space Agency (STAR project 182-OANA) and the Belgian Solar Terrestrial Center of Excellence (STCE). SF is supported by JSPS KAKENHI Grant Number JP17K05671. DJK is supported by the National Sciences and Engineering Council of Canada. RLL is supported by NSF grant AGS-1558134. OM acknowledges support by SIFACIT contract 4000118383/16/I–EF with ESA and STAR EXPRESS contract 119/2017 with Romanian Space Agency. THW is supported by JSPS KAKENHI Grant Number JP16H04086 and JP17H01177. The authors also wish to thank the International Space Science Institute ISSI-Bern for organization of this review and for financial support of the team meeting.

Appendix: Some Theories of Auroral Arc Generation that Are in Disuse

Some auroral-arc generator models that were reviewed previously (Borovsky 1993) are no longer actively discussed in the literature. These theories are briefly outlined below.

Arcs Generated at Reconnection *X*-Lines Atkinson (1992) argued that auroral arcs magnetically connect to reconnection *X*-lines where they are driven by charge-separation electric fields produced by the differences in electron and ion inertia in the plasma flow through the reconnection diffusion region (i.e. collisionless Hall effects). He further argued (Atkinson et al. 1989) that multiple auroral arcs map to multiple reconnection *X*-lines in the magnetotail (see also Safargaleev et al. 1997).

Arcs Generated on a Resonant Absorption Layer The idea was discussed (Hasegawa 1976; Goertz 1984) wherein kinetic Alfvén waves could be driven by mode conversion on a resonant layer in the magnetotail and that the kinetic Alfvén waves could accelerate electrons into the atmosphere to produce an auroral arc. The energy source most discussed was MHD surface waves (e.g. Kelvin-Helmholtz waves) on the magnetopause driven by the solar wind, with the evanescent surface waves mode converting on density boundaries in the plasma sheet. One drawback with this idea is that the magnetospheric surface waves are traveling antisunward and they will mode convert to produce kinetic Alfvén waves that are propagating antisunward, opposite to the Alfvén waves observed to accelerate electrons sunward (Earthward) to produce aurora. Chen and Kivelson (1991) evaluated the amplitudes of ULF MHD waves in the lobe (between the magnetopause surface wave and the plasma sheet) and found the power transport to be weak (see also the comments of Keiling (2009)). Note that ideas about mode conversion from solar-wind-driven waves to Alfvén waves that drive the aurora are active (cf. Sect. 2.1), with the solar-wind-driven waves being magnetosonic waves instead of Kelvin-Helmholtz waves.

Arcs Generated by Earthward Ion or Plasma Streams Driving Electrostatic Shocks Ideas were presented (e.g. Kan 1975; Kan and Akasofu 1976) wherein observed Earthward streams of ions (or plasma flows) in the high-latitude portions of the plasma sheet could drive electrostatic shocks (e.g. Swift 1976) near the Earth that stopped the Earthward ion flow and accelerated electrons Earthward to produce auroral arcs. In this picture the power for the auroral arc came from the ram kinetic energy of the Earthward moving ions. The conversion of the ion flow energy into electron beam energy by an electrostatic potential structure has not recently been discussed in the literature, although the conversion of ion-beam energy into Alfvén waves via firehose-type instabilities has been discussed (cf. Sect. 2.1).

Arcs Generated by Earthward Ion Streams Driving Lower-Hybrid Waves Lower-hybrid waves can transfer energy between ions and electrons. A model for high-latitude auroral arcs was suggested in which Earthward streams of ions in the plasma sheet boundary layer could drive a turbulence of lower-hybrid waves, which in turn stochastically accelerated electrons toward the atmosphere to produce auroral arcs (Bingham et al. 1984, 1988; Roy and Lakhina 1985; Bryant 1990; Bryant et al. 1991). Analogous to the prior model, this idea has not been discussed recently in the literature.

Plasma-Sheet Flow Turbulence Inverse Cascading to Form an Arc For MHD turbulence restricted to two dimensions there was a plasma-physics research focus on an inverse cascade of turbulent energy to large spatial scales (Fyfe et al. 1977; Pouquet 1978). In magnetospheric physics several calculations and simulations focused on the idea of two-dimensional MHD or electrostatic $\underline{E} \times \underline{B}$ turbulence in the plasma sheet undergoing an inverse energy cascade to form a coherent structure, mapping to an east-west-aligned auroral arc (Swift 1977, 1979, 1981; Lotko and Schultz 1988; Song and Lysak 1988).

References

S.-I. Akasofu, The development of the auroral substorm. Planet. Space Sci. **12**, 273 (1964)

S.-I. Akasofu, Recent progress in studies of DMSP auroral photographs. Space Sci. Rev. **19**, 169 (1976)

V. Angelopoulos, C.F. Kennell, F.V. Coroniti, R. Pellat, H.E. Spence, M.G. Kivelson, R.J. Walker, W. Baumjohann, W.C. Feldman, J.T. Gosling, C.T. Russell, Characteristics of ion flow in the quiet state of the inner plasma sheet. Geophys. Res. Lett. **20**, 1711 (1993)

V. Angelopoulos, C.F. Kennell, F.V. Coroniti, R. Pellat, M.G. Kivelson, R.J. Walker, C.T. Russell, W. Baumjohann, W.C. Feldman, J.T. Gosling, Statistical characteristics of bursty bulk flow events. J. Geophys. Res. **99**, 21257 (1994)

E.E. Antonova, M.V. Stepanova, M.V. Teltzov, B.A. Tverskoy, Multiple inverted-V structures and hot plasma pressure gradient mechanism of plasma stratification. J. Geophys. Res. **103**, 9317 (1998)

G. Atkinson, Auroral arcs: result of the interaction of a dynamic magnetosphere with the ionosphere. J. Geophys. Res. **75**, 4746 (1970)

G. Atkinson, Review of auroral currents and auroral arcs. J. Geomagn. Geoelectr. **30**, 435 (1978)

G. Atkinson, Mechanism by which merging at *X* lines causes discrete auroral arcs. J. Geophys. Res. **97**, 1337 (1992)

G. Atkinson, F. Creutzberg, R.L. Gattinger, J.S. Murphree, Interpretation of complicated discrete arc structure and behavior in terms of multiple *X* lines. J. Geophys. Res. **94**, 5292 (1989)

N.G. Aunai, G. Belmont, R. Smets, Energy budgets in collisionless magnetic reconnection: ion heating and bulk acceleration. Phys. Plasmas **18**, 122901 (2011)

R. Bingham, D.A. Bryant, D.S. Hall, A wave model for the aurora. Geophys. Res. Lett. **11**, 327 (1984)

R. Bingham, D.A. Bryant, D.S. Hall, Auroral electron acceleration by lower-hybrid waves. Ann. Geophys. **6**, 159 (1988)

J. Birn, Three-dimensional equilibria for the extended magnetotail and the generation of field-aligned current sheets. J. Geophys. Res. **94**, 252 (1989)

J. Birn, M. Hesse, The substorm current wedge and field-aligned currents in MHD simulations of magnetotail reconnection. J. Geophys. Res. **96**, 1611 (1991)

J. Birn, M. Hesse, Energy release and conversion by reconnection in the magnetotail. Ann. Geophys. **23**, 3365 (2005)

J. Birn, M. Hesse, The substorm current wedge in MHD simulations. J. Geophys. Res. **118**, 3364 (2013)

J. Birn, M. Hesse, The substorm current wedge: further insights from MHD simulations. J. Geophys. Res. Space Phys. **119**, 3503 (2014)

J. Birn, M. Hesse, G. Haerendel, W. Baumjohann, K. Shiokawa, Flow braking and the substorm current wedge. J. Geophys. Res. **104**, 19895 (1999)

J. Birn, J.F. Drake, M.A. Shay, B.N. Rogers, R.E. Denton, M. Hesse, M. Kuznetsova, Z.W. Ma, A. Bhattacharjee, A. Otto, P.L. Pritchett, Geospace Environment Modeling (GEM) magnetic reconnection challenge. J. Geophys. Res. **106**, 3715 (2001)

J. Birn, K. Schindler, M. Hesse, Thin electron current sheets and their relation to auroral potentials. J. Geophys. Res. **109**, A02217 (2004a)

J. Birn, J. Raeder, Y.L. Wang, R.A. Wolf, M. Hesse, On the propagation of bubbles in the geomagnetic tail. Ann. Geophys. **22**, 1773 (2004b)

J. Birn, R. Nakamura, E. Panov, M. Hesse, Bursty bulk flows and dipolarization in MHD simulations of magnetotail reconnection. J. Geophys. Res. **116**, A01210 (2011)

J. Birn, K. Schindler, M. Hesse, Magnetotail aurora connection: the role of thin current sheets. Geophys. Monogr. Ser. **197**, 337 (2012)

J. Birn, M. Hesse, A. Runov, X.-Z. Zhou, Ion beams in the plasma sheet boundary layer. J. Geophys. Res. **120**, 7522 (2015)

M.G. Bobra, S. Ilonidis, Predicting coronal mass ejections using machine learning methods. Astrophys. J. **821**, 127 (2016)

J.E. Borovsky, Auroral arc thicknesses as predicted by various theories. J. Geophys. Res. **98**, 6101 (1993)

J.E. Borovsky, The Magnetosphere-Ionosphere Observatory (MIO). Los Alamos National Laboratory (2002). https://www.lanl.gov/csse/MIOwriteup.pdf

J.E. Borovsky, J. Birn, The solar-wind electric field does not control the dayside reconnection rate. J. Geophys. Res. **119**, 751 (2014)

J.E. Borovsky, J.L. Delzanno, Space active experiments: the future. Front. Astron. Space Sci. **6**, 31 (2019)

J.E. Borovsky, H.O. Funsten, MHD turbulence in the Earth's plasma sheet: dynamics, dissipation, and driving. J. Geophys. Res. **108**, 1284 (2003)

J.E. Borovsky, J.A. Valdivia, The Earth's magnetosphere: a systems science overview and assessment. Surv. Geophys. **39**, 817 (2018)

J.E. Borovsky, R.C. Elphic, H.O. Funsten, M.F. Thomsen, The Earth's plasma sheet as a laboratory for turbulence in high-beta MHD. J. Plasma Phys. **57**, 1 (1997)
J.E. Borovsky, M.F. Thomsen, R.C. Elphic, The driving of the plasma sheet by the solar wind. J. Geophys. Res. **103**, 17617 (1998a)
J.E. Borovsky, M.F. Thomsen, D.J. McComas, T.E. Cayton, D.J. Knipp, Magnetospheric dynamics and mass flow during the November-1993 storm. J. Geophys. Res. **103**, 26373 (1998b)
J.E. Borovsky, R.A. Greenwald, T.J. Hallinan, J.L. Horwitz, M.C. Kelley, D.M. Klumpar, R.L. Lysak, B.H. Mauk, T.M. Moore, G.D. Reeves, H.J. Singer, M.F. Thomsen, The magnetosphere-ionosphere facility: a satellite cluster in geosynchronous orbit connected to ground-based observatories. Eos **79**(45), F744 (1998c)
J.M. Bosqued, M. Ashour-Abdalla, M. El Alaoui, V. Peroomian, L.M. Zelenyi, C.P. Escoubet, Dispersed ion structures at the poleward edge of the auroral oval: low-altitude observations and numerical modeling. J. Geophys. Res. **98**, 19181 (1993)
R. Boström, A model of the auroral electrojets. J. Geophys. Res. **69**, 4983 (1964)
J.S. Boyd, A.E. Belon, G.J. Romick, Latitude and time variations in precipitated electron energy inferred from measurements of auroral heights. J. Geophys. Res. **76**, 7694 (1971)
P.C. Brandt, S.Y. Hsieh, R. DeMajistre, D.G. Mitchell, ENA imaging of planetary ring currents. Geophys. Monogr. Ser. **235**, 95 (2018)
D.A. Bryant, Auroral electron acceleration. Phys. Scr. T **30**, 215 (1990)
D.A. Bryant, A.C. Cook, Z.-S. Wang, U. de Angelis, C.H. Perry, Turbulent acceleration of auroral electrons. J. Geophys. Res. **96**, 13829 (1991)
J. Buechner, L.M. Zeleny, Deterministic chaos in the dynamics of charged particles near a magnetic field reversal. Phys. Lett. A **118**, 395 (1986)
J. Buechner, L.M. Zelenyi, Regular and chaotic charged particle motion in magnetotaillike field reversals. I—Basic theory of trapped motion. J. Geophys. Res. **94**, 11,821 (1989)
W.J. Burke, J.S. Machuzak, N.C. Maynard, E.M. Basinski, G.M. Erickson, R.A. Hoffman, J.A. Slavin, W.B. Hanson, Auroral ionospheric signatures of the plasma sheet boundary layer in the evening sector. J. Geophys. Res. **99**, 2489 (1994)
E. Camporeale, S. Wing, J. Johnson, *Machine Learning Techniques for Space Weather* (Elsevier, Amsterdam, 2018)
J. Cao, Y. Ma, G. Parks, H. Reme, I. Dandouras, T. Zhang, Kinetic analysis of the energy transport of busty bulk flows in the plasma sheet. J. Geophys. Res. **118**, 313 (2013)
C.A. Cattell, F.S. Mozer, Electric fields measured by ISEE-1 within and near the neural sheet during quiet and active times. Geophys. Res. Lett. **9**, 1041 (1982)
C.C. Chaston, L.M. Peticolas, J.W. Bonnell, C.W. Carlson, R.E. Ergun, J.P. McFadden, R.J. Strangeway, Width and brightness of auroral arcs driven by inertial Alfvén waves. J. Geophys. Res. **198**, 1091 (2003)
S.-H. Chen, M.G. Kivelson, On ultralow frequency waves in the lobes of the Earth's magnetotail. J. Geophys. Res. **96**, 15711 (1991)
I.J. Cohen et al., Auroral Current and Electrodynamics Structure (ACES) observations of ionospheric feedback in the Alfvén resonator and model responses. J. Geophys. Res. Space Phys. **118**, 3288 (2013)
F.V. Coroniti, P.L. Pritchett, The quiet evening auroral arc and the structure of the growth phase near-Earth plasma sheet. J. Geophys. Res. **119**, 1827 (2014)
National Research Council, Magnetosphere-to-ionosphere field-line tracing technology, in *Solar and Space Physics: A Science for a Technological Society* (National Academies Press, Washington, D.C., 2012), p. 333
J. De Keyser, M. Echim, Auroral and sub-auroral phenomena: an electrostatic picture. Ann. Geophys. **28**, 633 (2010)
J. De Keyser, M. Echim, Electric potential differences across auroral generator interfaces. Ann. Geophys. **31**, 251 (2013)
J. De Keyser, R. Maggiolo, M. Echim, Monopolar and bipolar auroral electric fields and their effects. Ann. Geophys. **28**, 2027 (2010)
G.L. Delzanno, J.E. Borovsky, M.F. Thomsen, B.E. Gilchrist, E. Sanchez, Can an electron gun solve the outstanding problem of magnetosphere-ionosphere connectivity? J. Geophys. Res. **121**, 6769 (2016)
I.S. Dmitrienko, Formation of accelerated ion flows in Alfvén disturbances of the magnetotail. Geomagn. Aeron. **51**, 1160 (2011)
E.F. Donovan, B.J. Jackel, I. Voronkov, T. Sotirelis, F. Creutzberg, N.A. Nicholson, Ground-based optical determination of the b2i boundary: a basis for an optical MT-index. J. Geophys. Res. **108**, 1115 (2003)
S.D. Drell, H.M. Foley, M.A. Ruderman, Drag and propulsion of large satellites in the ionosphere: an Alfvén propulsion engine in space. Phys. Rev. Lett. **14**, 171 (1965)
J.P. Eastwood, T.D. Phan, J.F. Drake, M.A. Shay, A.L. Borg, B. Lavraud, M.G.G.T. Taylor, Energy partition in magnetic reconnection in Earth's magnetotail. Phys. Rev. Lett. **110**, 225001 (2013)

R.H. Eather, *Majestic Lights: The Aurora in Science, History, and the Arts* (American Geophysical Union Press, Washington, 1980)
Y. Ebihara, T. Tanaka, Substorm simulation: insight into the mechanisms of initial brightening. J. Geophys. Res. Space Phys. **120**, 7270 (2015a)
Y. Ebihara, T. Tanaka, Substorm simulation: formation of westward traveling surge. J. Geophys. Res. Space Phys. **120**, 10466 (2015b)
Y. Ebihara, T. Tanaka, Substorm simulation: quiet and N-S arcs preceding auroral breakup. J. Geophys. Res. Space Phys. **121**, 1201 (2016)
Y. Ebihara, T. Tanaka, Energy flow exciting field-aligned current at substorm expansion onset. J. Geophys. Res. **122**, 12288 (2017)
M.M. Echim, M. Roth, J. de Keyser, Sheared magnetospheric plasma flows and discrete auroral arcs: a quasi-static coupling model. Ann. Geophys. **25**, 317 (2007)
M.M. Echim, M. Roth, J. de Keyser, Ionospheric feedback effects on the quasi-stationary coupling between LLBL and postnoon/evening discrete auroral arcs. Ann. Geophys. **26**, 913 (2008)
M.M. Echim, R. Maggiolo, M. Roth, J. De Keyser, A magnetospheric generator driving ion and electron acceleration and electric currents in a discrete auroral arc observed by Cluster and DMSP. Geophys. Res. Lett. **36**, L12111 (2009)
M. El-Alaoui, R.L. Richard, M. Ashour-Abdalla, R.J. Walker, M.L. Goldstein, Turbulence in a global magnetohydrodynamic simulation of the Earth's magnetosphere during northward and southward interplanetary magnetic field. Nonlinear Process. Geophys. **19**, 165 (2012)
R.C. Elphic et al., The auroral current circuit and field-aligned currents observed by FAST. Geophys. Res. Lett. **25**, 2033 (1998)
R.C. Elphic, M.F. Thomsen, J.E. Borovsky, D.J. McComas, Inner edge of the electron plasma sheet: empirical models of boundary location. J. Geophys. Res. **104**, 22679 (1999)
R.D. Elphinstone, D. Hearn, J.S. Murphree, L.L. Cogger, Mapping using the Tsyganenko Long magnetospheric model and its relationship to Viking auroral images. J. Geophys. Res. **96**, 1467 (1991)
Y.I. Feldstein, Y.I. Galperin, The auroral luminosity structure in the high-latitude upper atmosphere: its dynamics and relationship to the large-scale structure of the Earth's magnetosphere. Rev. Geophys. **23**, 217 (1985)
S.M. Finnegan, M.E. Koepke, D.J. Knudsen, The dispersive Alfvén wave in the time-stationary limit with a focus on collisional and warm-plasma effects. Phys. Plasmas **15**, 052108 (2008)
D. Fyfe, D. Montgomery, G. Joyce, Dissipative, forced turbulence in two-dimensional magnetohydrodynamics. J. Plasma Phys. **17**, 369 (1977)
Y.I. Galperin, J.M. Bosqued, Stationary magnetospheric convection on November 24, 1981. 1. A case study of "pressure gradient/minimum-B" auroral arc generation. Ann. Geophys. **17**, 358 (1999)
Y.I. Galperin, Y.I. Feldstein, Mapping the precipitation regions to the plasma sheet. J. Geomagn. Geoelectr. **48**, 857 (1996)
Y.I. Galperin, A.V. Volosevich, L.M. Zelenyi, Pressure gradient structures in the tail neutral sheet as "roots of the arcs" with some effects of stochasticity. Geophys. Res. Lett. **19**, 2163 (1992)
Y.S. Ge, J. Raeder, V. Angelopoulos, M.L. Gilson, A. Runov, Interaction of dipolarization fronts within multiple bursty bulk flows in global MHD simulations of a substorm on 27 February 2009. J. Geophys. Res. **116**, A00123 (2011)
D.M. Gillies, D. Knudsen, E. Donovan, B. Jackel, R. Gillies, E. Spanswick, Identifying the 630 nm auroral arc emission height: a comparison of the triangulation, FAC profile, and electron density methods. J. Geophys. Res. **122**, 8181 (2017)
D.M. Gillies, D. Knudsen, R. Rankin, S. Milan, E. Donovan, A statistical survey of the 630.0-nm optical signature of periodic auroral arcs resulting from magnetospheric field line resonances. Geophys. Res. Lett. **45**, 4648 (2018)
C.K. Goertz, Alfvén waves on auroral field lines. Planet. Space Sci. **32**, 1387 (1984)
C.K. Goertz, R.W. Boswell, Magnetosphere-ionosphere coupling. J. Geophys. Res. **84**, 7239 (1979)
H. Grad, Some new variational properties of hydromagnetic equilibria. Phys. Fluids **7**, 1283 (1964)
E.E. Grigorenko, J.-A. Sauvaud, L.M. Zelenyi, Spatial-temporal characteristics of ion beamlets in the plasma sheet boundary layer of magnetotail. J. Geophys. Res. **112**, A05218 (2007)
D.A. Gurnett, C.K. Goertz, Multiple Alfvén wave reflections excited by Io: origin of the Jovain decametric arcs. J. Geophys. Res. **86**, 717 (1981)
M.S. Gussenhoven, D.A. Hardy, W.J. Burke, DMSP/F2 electron observations of equatorward auroral boundaries an their relationship to magnetospheric electric fields. J. Geophys. Res. **86**, 768 (1981)
M.S. Gussenhoven, D.A. Hardy, N. Heinemann, Systematics of the equatorward diffuse auroral boundary. J. Geophys. Res. **88**, 5692 (1983)
G. Haerendel, Acceleration from field-aligned potential drops. Astrophys. J. Suppl. Ser. **90**, 765 (1994)

G. Haerendel, Outstanding issues in understanding the dynamics of the inner plasma sheet and ring current during storms and substorms. Adv. Space Res. **25**, 2379 (2000)
G. Haerendel, Auroral arcs as sites of magnetic stress release. J. Geophys. Res. **112**, A09214 (2007)
G. Haerendel, Auroral arcs as current transformers. J. Geophys. Res. **113**, A07205 (2008)
G. Haerendel, Poleward arcs of the auroral oval during substorms and the inner edge of the plasma sheet. J. Geophys. Res. **114**, A06214 (2009)
G. Haerendel, Equatorward moving arcs and substorm onset. J. Geophys. Res. **115**, A07212 (2010)
G. Haerendel, Six auroral generators: a review. J. Geophys. Res. **116**, A00K05 (2011)
G. Haerendel, A tool for characterizing and evaluating Type II auroral arcs. J. Geophys. Res. **117**, A06214 (2012a)
G. Haerendel, Auroral generators: a survey. Geophys. Monogr. Ser. **197**, 347 (2012b)
G. Haerendel, S. Buchert, C. La Hoz, B. Raaf, E. Rieger, On the proper motion of auroral arcs. J. Geophys. Res. **98**, 6087 (1993)
T.J. Hallinan, *The Distribution of Vorticity in Auroral Arcs*. Geophys. Res. Monogr., vol. 25, (1981), p. 42
M. Hamrin, P. Norqvist, O. Marghitu, S. Buchert, B. Klecker, L.M. Kistler, I. Dandouras, Occurrence and location of concentrated load and generator regions observed by Cluster in the plasma sheet. Ann. Geophys. **27**, 4131 (2009)
M. Hamrin, O. Marghitu, P. Norqvist, S. Buchert, M. Andre, B. Klecker, L.M. Kistler, I. Danouras, Energy conversion regions as observed by Cluster in the plasma sheet. J. Geophys. Res. **116**, A00K8 (2011)
P.J. Hanson, B.G. Harrold, Parallel inhomogeneity and the Alfvén resonance 1. Open field lines. J. Geophys. Res. **99**, 2429 (1994)
B.G. Harrold, C.K. Goertz, R.A. Smith, P.J. Hansen, Resonant Alfvén wave heating of the plasma sheet boundary layer. J. Geophys. Res. **95**, 15039 (1990)
A. Hasegawa, Particle acceleration by MHD surface wave and formation of aurora. J. Geophys. Res. **81**, 5083 (1976)
A. Hasegawa, T. Sato, Generation of field aligned current during substorm, in *Dynamics of the Magnetosphere*, ed. by S.-I. Akasofu (D. Reidel Publishing, Dordrecht, 1979), p. 529
M. Henderson, Observational evidence for an inside-out substorm onset scenario. Ann. Geophys. **27**, 2120 (2009)
M. Hesse, D. Winske, M. Kuznetsova, J. Birn, K. Schindler, Hybrid modeling of the formation of thin current sheets in magnetotail configurations. J. Geomagn. Geoelectr. **48**, 749 (1996)
M. Hesse, D. Winske, J. Birn, On the ion-scale structure of thin current sheets in the magnetotail. Phys. Scr. T **74**, 63 (1998)
Y. Hiraki, T. Watanabe, Feedback instability analysis for dipole configuration with ionospheric and magnetospheric cavities. J. Geophys. Res. **116**, A11220 (2011)
Y. Hiraki, T.-H. Watanabe, Hybrid Alfvén resonant mode generation in the magnetosphere-ionosphere coupling system. Phys. Plasmas **19**, 102904 (2012)
M.-S. Hsieh, A. Otto, The influence of magnetic flux depletion on the magnetotail and auroral morphology during the substorm growth phase. J. Geophys. Res. **119**, 3430 (2014)
T. Iijima, T.A. Potemra, Large-scale characteristics of field-aligned currents associated with substorms. J. Geophys. Res. **83**, 599 (1978)
N. Jia, A.V. Streltsov, Ionospheric feedback instability and active discrete auroral forms. J. Geophys. Res. **119**, 2243 (2014)
F. Jiang, M.G. Kivelson, R.J. Strangeway, K.K. Khurana, R. Walker, Ionospheric flow shear associated with the preexisting auroral arc: a statistical study from the FAST spacecraft data. J. Geophys. Res. Space Phys. **120**, 5194 (2015)
A. Kadokura, A.-S. Yukimatu, M. Ejiri, T. Oguti, M. Pinnock, M.R. Hairston, Detailed analysis of a substorm event on 6 and 7 June 1989, 1, growth phase evolution of nightside auroral activities and ionospheric convection toward expansion phase onset. J. Geophys. Res. **107**, 1479 (2002)
J. Kan, Energization of auroral electrons by electrostatic shock-waves. J. Geophys. Res. **80**, 2089 (1975)
J.R. Kan, S.-I. Akasofu, Energy source and mechanisms for accelerating the electrons and driving the field-aligned currents for the discrete auroral arc. J. Geophys. Res. **81**, 5123 (1976)
T. Karlsson, L. Andersson, M. Gillies, K. Lynch, O. Marghitu, N. Partamies, N. Sivadas, J. Wu, Quiet, discrete arcs—observations. Space Sci. Rev. (2019, submitted)
A. Keiling, Alfvén waves and their roles in the dynamics of the Earth's magnetotail: a review. Space Sci. Rev. **142**, 73 (2009)
A. Keiling, G.K. Parks, H. Reme, I. Dandouras, M. Wilber, L. Distler, C. Owen, A.N. Fazakerley, E. Lucek, M. Maksimovic, N. Cornilleau-Wehrlin, Energy-dispersed ions in the plasma sheet boundary layer and associated phenomena: ion heating, electron acceleration, Alfvén waves, broadband waves, perpendicular electric field spikes, and auroral emissions. Ann. Geophys. **24**, 2685 (2006)

A. Keiling et al., Substorm current wedge driven by plasma flow vortices: THEMIS observations. J. Geophys. Res. **114**, A00C22 (2009)
M.C. Kelley, C.W. Carlson, Observations of intense velocity shear and associated electrostatic waves near an auroral arc. J. Geophys. Res. **82**, 2343 (1977)
J.S. Kim, R.A. Volkman, Thickness of zenithal auroral arc over Fort Churchill, Canada. J. Geophys. Res. **68**, 3187 (1963)
C.A. Kletzing, Electron acceleration by kinetic Alfvén waves. J. Geophys. Res. **99**, 11095 (1994)
L. Knight, Parallel electric fields. Planet. Space Sci. **21**, 741 (1973)
D.J. Knudsen, Spatial modulation of electron energy and density by nonlinear stationary inertial Alfvén waves. J. Geophys. Res. **101**, 10761 (1996)
D.J. Knudsen, E.F. Donovan, L.L. Cogger, B. Jackel, W.D. Shaw, Width and structure of mesoscale optical auroral arcs. Geophys. Res. Lett. **28**, 705 (2001)
D.J. Knudsen, J.K. Burchill, E.F. Donovan, V.M. Uritsky, Advection of magnetic energy as a source of power for auroral arcs. Geophys. Res. Lett. **38**, L24103 (2011)
G. Kremser, A. Korth, S.L. Ullaland, S. Perraut, A. Roux, A. Pedersen, R. Schmidt, P. Tanskanen, Field-aligned beams of energetic electrons (16 keV $< E <$ 80 keV) observed at geosynchronous orbit at substorm onset. J. Geophys. Res. **93**, 14453 (1988)
M. Kubyshkina, V. Sergeev, N. Tsyganenko, V. Angelopoulos, A. Runov, E. Donovan, H. Singer, U. Auster, W. Baumjohann, Time-dependent magnetospheric configuration and breakup mapping during a substorm. J. Geophys. Res. **116**, A00I27 (2011)
J. Lemaire, M. Scherer, Plasma sheet particle precipitation: a kinetic model. Planet. Space Sci. **21**, 281 (1973)
J. Liang, E.F. Donovan, W.W. Liu, B. Jackel, M. Syrjäsuo, S.B. Mende, H.U. Frey, V. Angelopoulos, M. Connors, Intensification of preexisting auroral arc at substorm expansion phase onset: wave-like disruption during the first tens of seconds. Geophys. Res. Lett. **35**, L17S19 (2008)
J. Liang, Y. Shen, D. Knudsen, E. Spanswick, J. Burchill, E. Donovan, e-POP and red line optical observations of Alfvénic aurora. J. Geophys. Res. **124**, 4672 (2019)
J. Liu, V. Angelopoulos, A. Runov, X.-Z. Zhou, On the current sheets surrounding dipolarizing flux bundles in the magnetotail: the case for wedgelets. J. Geophys. Res. Space Phys. **118**, 2000 (2013)
W. Lotko, C.G. Schultz, Internal shear layers in auroral dynamics. Geophys. Monogr. Ser. **44**, 121 (1988)
W. Lotko, B.U.O. Sonnerup, R.L. Lysak, Nonsteady boundary layer flow including ionospheric drag and parallel electric fields. J. Geophys. Res. **92**, 8635 (1987)
G. Lu, M. Brittnacher, G. Parks, D. Lummerzheim, On the magnetospheric source regions of substorm-related field-aligned currents and auroral precipitation. J. Geophys. Res. **105**, 18483 (2000)
J.Y. Lu, R. Rankin, R. Marchand, I.J. Rae, W. Wang, S.C. Solomon, J. Lei, Electrodynamics of magnetosphere-ionosphere coupling and feedback on magnetospheric field line resonances. J. Geophys. Res. **112**, A10219 (2007)
J.Y. Lu, W. Wang, R. Rankin, R. Marchand, J. Lei, S.C. Solomon, I.J. Rae, J.-S. Wang, G.-M. Le, Electromagnetic waves generated by ionospheric feedback instability. J. Geophys. Res. **113**, A05206 (2008)
R. Lundin, D.S. Evans, Boundary layer plasmas as a source for high-latitude, early afternoon, auroral arcs. Planet. Space Sci. **32**, 1389 (1985)
R. Lundin, I. Sandahl, Some characteristics of the parallel electric field acceleration of electrons over discrete auroral arcs as observed from two rocket flights. Tech. Rep. SP-135, European Space Agency (1978)
L.R. Lyons, Generation of large-scale regions of auroral currents, electric potentials and precipitation by the divergence of the convection electric field. J. Geophys. Res. **85**, 17 (1980)
L.R. Lyons, Discrete aurora as the direct result of an inferred high-altitude generating potential distribution. J. Geophys. Res. **86**, 1 (1981)
L.R. Lyons, D.S. Evans, An association between discrete aurora and energetic particle boundaries. J. Geophys. Res. **89**, 2395 (1984)
L.R. Lyons, T.W. Speiser, Evidence for current sheet acceleration in the geomagnetic tail. J. Geophys. Res. **87**, 2276 (1982)
L.R. Lyons, D.S. Evans, R. Lundin, An observed relation between magnetic field aligned electric fields and downward electron energy fluxes in the vicinity of auroral forms. J. Geophys. Res. **84**, 457 (1979)
R.L. Lysak, Auroral electrodynamics with current and Voltage generators. J. Geophys. Res. **90**, 4178 (1985)
R.L. Lysak, Feedback instability of the ionospheric resonant cavity. J. Geophys. Res. **96**, 1553–1568 (1991)
R.L. Lysak, Y. Song, Energetics of the ionospheric feedback interaction. J. Geophys. Res. **107**, 1160 (2002)
R.L. Lysak, Y. Song, Development of parallel electric fields at the plasma sheet boundary layer. J. Geophys. Res. **116**, A00K14 (2011)
R.L. Lysak, Y. Song, T.W. Jones, Propagation of Alfvén waves in the magnetotail during substorms. Ann. Geophys. **27**, 2237 (2009)

R. Maggiolo, M. Echim, C.S. Wedlund, Y. Zhang, D. Fontaine, G. Lointier, J.-G. Trotignon, Polar cap arcs from the magnetosphere to the ionosphere: kinetic modelling and observations by Cluster and TIMED. Ann. Geophys. **30**, 283 (2012)
A.J. Mallinckrodt, C.W. Carlson, Relations between transverse electric fields and field-aligned currents. J. Geophys. Res. **83**, 1426 (1978)
Y.P. Maltsev, W.B. Lyatsky, A.M. Lyatskaya, Currents over the Auroral Arc. Planet. Space Sci. **25**, 53 (1977)
O. Marghitu, B. Klecker, G. Haerendel, J. McFadden, ALADYN: a method to investigate auroral arc electrodynamics from satellite data. J. Geophys. Res. **109**(A11), 305 (2004)
O. Marghitu, T. Karlsson, B. Klecker, G. Haerendel, J. McFadden, Auroral arc and oval electrodynamics in the Harang region. J. Geophys. Res. **114**, A03214 (2009)
O. Marghitu, M. Hamrin, B. Klecker, K. Ronnmak, S. Buchert, L.M. Kistler, M. Andre, H. Reme, Cluster observations of energy conversion regions in the plasma sheet, in *The Cluster Active Archive*, ed. by H. Laakso et al. (Springer, Berlin, 2010)
O. Marghitu, C. Bunescu, T. Karlsson, B. Klecker, On the divergence of the auroral electrojets. J. Geophys. Res. **116**, A00K17 (2011)
G. Marklund, Auoral arc classification scheme based on the observed arc-associated electric field pattern. Planet. Space Sci. **32**, 193 (1984)
G.T. Marklund et al., Cluster multipoint study of the acceleration potential pattern and electrodynamics of an auroral surge and its associated horn arc. J. Geophys. Res. **117**, A10223 (2012)
B.H. Mauk, C.-I. Meng, The aurora and middle magnetospheric processes, in *Auroral Physics*, ed. by C.-I. Meng, M.J. Rycroft, L.A. Frank (Cambridge Press, Cambridge, 1991), p. 223
R.M. McGranaghan, A.J. Manucci, B. Wilson, C.A. Mattmann, R. Chadwick, New capabilities for prediction of high-latitude ionospheric scintillation: a novel approach with machine learning. Space Weather **16**, 1817 (2018)
C.E. McIlwain, Auroral electron beams near the magnetic equator, in *Physics of the Hot Plasma in the Magnetosphere*, ed. by B. Hultqvist, L. Stenflo (Plenum, New York, 1975), p. 91
R.L. McPherron, C.T. Russell, M.P. Aubry, Satellite studies of magnetospheric substorms on August 15, 1968, 9, phenomenological model for substorms. J. Geophys. Res. **78**, 3131 (1973)
R.L. McPherron, A. Nishida, C.T. Russell, Is near-Earth current sheet thinning the cause of substorm onset? in *Quantitative Modeling of Magnetosphere-Ionosphere Coupling Processes*, ed. by Y. Kamide, R.A. Wolf (Kyoto Sangyo University, Kyoto, 1987), p. 252
C.-I. Meng, B. Mauk, C.E. McIlwain, Electron precipitation of evening diffuse aurora and its conjugate electron fluxes near the magnetospheric equator. J. Geophys. Res. **84**, 2545 (1979)
A. Miura, T. Sato, Numerical simulation of global formation of auroral arcs. J. Geophys. Res. **85**, 73 (1980)
T. Motoba, K. Hosokawa, A. Kadodura, N. Sato, Magnetic conjugacy of northern and southern auroral beads. Geophys. Res. Lett. **39**, L08101 (2012)
T. Motoba, S. Ohtani, B.J. Anderson, H. Korth, D. Mitchell, L.J. Lanzerotti, K. Shiokawa, M. Connors, C.A. Kletzing, G.D. Reeves, On the formation and origin of substorm growth phase/onset auroral arcs inferred from conjugate space-ground observations. J. Geophys. Res. **120**, 8707 (2015)
NASA, Sun-Earth Connection Roadmap 2003–2028, p. 92, http://www.dept.aoe.vt.edu/~cdhall/courses/aoe4065/NASADesignSPs/SEC_2003_roadmap_full.pdf (2003)
P.T. Newell, J.W. Gjerloev, SuperMAG-based partial ring current indices. J. Geophys. Res. **117**, A05215 (2012)
P.T. Newell, C.-I. Meng, K.M. Lyons, Suppression of discrete aurorae by sunlight. Nature **381**, 766 (1996a)
P.T. Newell, Y.I. Feldstein, Y.I. Galperin, C.-I. Meng, Morphology of nightside precipitation. J. Geophys. Res. **101**, 10,737 (1996b)
P.T. Newell, T. Sotirelis, S. Wing, Diffuse, monoenergetic, and broadband aurora: the global precipitation budget. J. Geophys. Res. **114**, A09207 (2009)
T.G. Onsager, T. Mukai, The structure of the plasma sheet and its boundary layers. J. Geomagn. Geoelectr. **48**, 687 (1996)
T.G. Onsager, M.F. Thomsen, R.C. Elphic, J.T. Gosling, Model of electron and ion distributions in the plasma sheet boundary layer. J. Geophys. Res. **96**, 20999 (1991)
N. Partamies, M. Syrjasuo, E. Donovan, M. Conners, D. Charrois, D. Knudsen, Z. Kryzanowsky, Observations of the auroral width spectrum at kilometer-scale size. Ann. Geophys. **29**, 711 (2010)
G. Paschmann, S. Haaland, R. Treumann, *Auroral Plasma Physics*. Space Sci. Rev., vol. 103 (2002)
A. Pedersen, C.A. Cattell, C.-G. Falthammar, K. Knott, P.-A. Lindqvist, R.H. Manka, F.S. Mozer, Electric fields I the plasma sheet and plasma sheet boundary layer. J. Geophys. Res. **90**, 1231 (1985)
A. Pouquet, On two-dimensional magnetohydrodynamic turbulence. J. Fluid Mech. **88**, 1 (1978)
P.L. Pritchett, Geospace Environment Modeling magnetic reconnection challenge: simulations with a full particle electromagnetic code. J. Geophys. Res. **106**, 3783 (2001)

P.L. Pritchett, F.V. Coroniti, Convection and the formation of thin current sheets in the near-Earth plasma sheet. Geophys. Res. Lett. **21**, 1587 (1994)
T.I. Pulkkinen, H.E.J. Koskinen, R.J. Pellinen, Mapping of auroral arcs during substorm growth phase. J. Geophys. Res. **96**, 21087 (1991)
T. Pulkkinen, D.N. Baker, D.G. Mitchell, R.L. McPherron, C.Y. Huang, L.A. Frank, Thin current sheets in the magnetotail during substorms: CDAW6 revisited. J. Geophys. Res. **99**, 5793 (1994)
J. Raeder, P. Zhu, Y. Ge, G. Siscoe, Auroral signatures of ballooning mode near substorm onset: open geospace general circulation model simulations. Geophys. Monogr. Ser. **197**, 389 (2012)
H. Rème, C. Aoustin, J.M. Bosqued, I. Dandouras, B. Lavraud, J.A. Sauvaud et al., First multispacecraft ion measurements in and near the Earth's magnetosphere with the identical Cluster Ion Spectrometry (CIS) experiment. Ann. Geophys. **19**, 1303 (2001)
G. Rostoker, On the place of the pseudo-breakup in a magnetospheric substorm. Geophys. Res. Lett. **25**, 217 (1998)
M. Roth, D.S. Evans, J. Lemaire, Theoretical structure of a magnetospheric plasma boundary: application to the formation of discrete auroral arcs. J. Geophys. Res. **98**, 11411 (1993)
M. Roth, J. De Keyser, M. Kuznetsova, Vlasov theory of the equilibrium structure of tangential discontinuities in space plasmas. Space Sci. Rev. **76**, 251 (1996)
M. Roy, G.S. Lakhina, Lower hybrid wave model for aurora. Astrophys. Space Sci. **117**, 111 (1985)
M.S. Ruderman, A.N. Wright, Excitation of resonant Alfvén waves in the magnetosphere by negative energy surface waves on the magnetopause. J. Geophys. Res. **103**, 26573 (1998)
V. Safargaleev, W. Lyatsky, V. Tagirov, Luminosity variations in several parallel auroral arcs before auroral breakup. Ann. Geophys. **15**, 959 (1997)
V.V. Safargaleev, A.E. Kozlovsky, S.V. Osipenko, V.R. Tagirov, Azimuthal expansion of high-latitude auroral arcs. Ann. Geophys. **21**, 1793 (2003)
J.C. Samson, L.L. Gogger, Q. Pao, Observations of field line resonances, auroral arcs, and auroral vortex structures. J. Geophys. Res. **101**, 17373 (1996)
P.B. Sandford, Variations of auroral emissions with time, magnetic activity and the solar cycle. J. Atmos. Terr. Phys. **30**, 1921 (1968)
J. Sanny, R.L. McPherron, C.T. Russell, D.N. Baker, T.I. Pulkkinen, A. Nishida, Growth-phase thinning of the near-Earth current sheet during the CDAW-6 substorm. J. Geophys. Res. **99**, 5805 (1994)
T. Sato, A theory of quiet auroral arcs. J. Geophys. Res. **83**, 1042 (1978)
T. Sato, T.E. Holzer, Quiet auroral arcs and electrodynamic coupling between the ionosphere and the magnetosphere, 1. J. Geophys. Res. **78**, 7314 (1973)
T. Sato, T. Iijima, Primary sources of large-scale Birkeland currents. Space Sci. Rev. **24**, 347 (1979)
N. Sato, T. Nagaoka, K. Hashimoto, T. Saemundsson, Conjugacy of isolated auroral arcs and nonconjugate auroral breakups. J. Geophys. Res. **103**, 11641 (1998)
K. Schindler, J. Birn, Magnetospheric physics. Phys. Rep. **47**, 109 (1978)
K. Schindler, J. Birn, Models of two-dimensional embedded thin current sheets from Vlasov theory. J. Geophys. Res. **107**, SMP20 (2002)
M. Scholer, A. Otto, Magnetotail reconnection: current diversion and field-aligned currents. Geophys. Res. Lett. **18**, 7331 (1991)
V.A. Sergeev, E.M. Sazhina, N.A. Tsyganenko, J.A. Lundblad, F. Soraas, Pitch-angle scattering of energetic protons in the magnetotail current sheet as the dominant source of their isotropic precipitation into the nightside ionosphere. Planet. Space Sci. **31**, 1147 (1983)
V.A. Sergeev, P. Tanskanen, K. Mursula, A. Korth, R.C. Elphic, Current sheet thickness in the near-Earth plasma sheet during substorm growth phase. J. Geophys. Res. **95**, 3819 (1990)
V.A. Sergeev, D.G. Mitchell, C.T. Russell, D.J. Williams, Structure of the tail plasma/current sheet at 11 R_E and its changes in the course of a substorm. J. Geophys. Res. **98**, 17345 (1993)
V.A. Sergeev, R.J. Pellinen, T.I. Pulkkinen, Steady magnetospheric convection: a review of recent results. Space Sci. Rev. **75**, 551 (1996)
V.A. Sergeev, J.-A. Sauvaud, D. Popescu, R.A. Kovrazhkin, K. Liou, P.T. Newell, M. Brittnacher, G. Parks, R. Nakarnura, T. Mukai, G.D. Reeves, Multiple-spacecraft observation of a narrow transient plasma jet in the Earth's plasma sheet. Geophys. Res. Lett. **27**, 851 (2000)
V. Sergeev, Y. Nishimura, M. Kubyshkina, V. Angelopoulos, R. Nakamura, H. Singer, Magnetospheric location of the equatorial prebreakup arc. J. Geophys. Res. **117**, A01212 (2012)
C.E. Seyler, A mathematical model of the structure and evolution of small-scale discrete auroral arcs. J. Geophys. Res. **95**, 17199 (1990)
I.G. Shevchenko, V. Sergeev, M. Kubyshkina, V. Angelopoulos, K.H. Glassmeier, H.J. Singer, Estimation of magnetosphere-ionosphere mapping accuracy using isotropy boundary and THEMIS observations. J. Geophys. Res. **115**, A11206 (2010)

R.A. Smith, C.K. Goertz, W. Grossmann, Thermal catastrophe in the plasma sheet boundary layer. Geophys. Res. Lett. **13**, 1380 (1986)
Y. Song, R.L. Lysak, Turbulent generation of auroral currents and fields—a spectral simulation of two-dimensional MHD turbulence. Geophys. Monogr. Ser. **44**, 197 (1988)
Y. Song, R.L. Lysak, Displacement current and the generation of parallel electric fields. Phys. Rev. Lett. **96**, 145002 (2006)
B.U.O. Sonnerup, Magnetic field reconnection, in *Solar System Plasma Physics*, vol. III, ed. by L.T. Lanzerotti, C.F. Kennel, E.N. Parker (North-Holland, New York, 1979), p. 45
B.U.O. Sonnerup, Theory of the low-latitude boundary layer. J. Geophys. Res. **85**, 2017 (1980)
K. Stasiewicz, Generation of magnetic-field aligned currents, parallel electric field, and inverted-V structures by plasma pressure inhomogeneities in the magnetosphere. Planet. Space Sci. **9**, 1037 (1985)
M.V. Stepanova, E.E. Antonova, G. Stanev, N. Bankov, N.V. Isaev, Study of stratification of magnetospheric convection using Intercosmos-Bulgaria-1300 electric field observations. Adv. Space Res. **31**, 1419 (2003)
M. Stepanova, V. Pinto, J.A. Valdivia, E.E. Antonova, Spatial distribution of the eddy diffusion coefficients in the plasma sheet during quiet time and substorms from THEMIS satellite data. J. Geophys. Res. **116**, A00I24 (2011)
R.J. Strangeway, The relationship between magnetospheric processes and auroral field-aligned current morphology. Geophys. Monogr. Ser. **197**, 355 (2012)
A.V. Streltsov, W. Lotko, Small-scale electric fields in the downward auroral current channels. J. Geophys. Res. **108**, 1289 (2003)
A.V. Streltsov, W. Lotko, Multiscale electrodynamics of the ionosphere-magnetosphere system. J. Geophys. Res. **109**, A09214 (2004)
A.V. Streltsov, W. Lotko, Coupling between density structures, electromagnetic waves and ionospheric feedback in the auroral zone. J. Geophys. Res. **113**, A05212 (2008)
A.V. Streltsov, E.V. Mishin, On the existence of ionospheric feedback instability in the Earth's magnetosphere-ionosphere system. J. Geophys. Res. **123**, 8951 (2018)
D.W. Swift, An equipotential model for auroral arcs 2. Numerical solutions. J. Geophys. Res. **81**, 3935 (1976)
D.W. Swift, Turbulent generation of electrostatic fields in the magnetosphere. J. Geophys. Res. **82**, 5143 (1977)
D.W. Swift, Mechanisms for the discrete aurora—a review. Space Sci. Rev. **22**, 35 (1978)
D.W. Swift, On the structure of auroral arcs: the results of numerical simulations. J. Geophys. Res. **84**, 469 (1979)
D.W. Swift, Numerical simulations of the generation of electrostatic turbulence in the magnetotail. J. Geophys. Res. **86**, 2273 (1981)
D. Sydorenko, R. Rankin, The stabilizing effect of collision-induced velocity shear on the ionospheric feedback instability in Earth's magnetosphere. Geophys. Res. Lett. **44**, 6534 (2017)
K. Takahashi, E.W. Hones, ISEE 1 and 2 observations of ion distributions at the plasma sheet-tail lobe boundary. J. Geophys. Res. **93**, 8558 (1988)
T. Tanaka, Generation mechanisms for magnetosphere—ionosphere current systems deduced from a three-dimensional MHD simulation of the solar wind-magnetosphere-ionosphere coupling processes. J. Geophys. Res. **100**, 12057 (1995)
T. Tanaka, Magnetosphere-ionosphere convection as a compound system. Space Sci. Rev. **133**, 1 (2007)
T. Tanaka, Substorm auroral dynamics reproduced by advanced global magnetosphere-ionosphere (M-I) coupling simulation. Geophys. Monogr. Ser. **215**, 177 (2015)
T. Tanaka, A. Nakamizo, A. Yoshikawa, S. Fujita, H. Shinagawa, H. Shimazu, T. Kikuchi, K.K. Hashimoto, Substorm convection and current system deduced from the global simulation. J. Geophys. Res. **115**, A05220 (2010)
T. Tanaka, Y. Ebihara, M. Watanabe, M. Den, S. Fujita, T. Kikuchi, K.K. Hashimoto, R. Kataoka, Global simulation study for the time sequence of events leading to the substorm onset. J. Geophys. Res. Space Phys. **122**, 6210 (2017)
T. Terasawa, Hall current effect on tearing mode instability. Geophys. Res. Lett. **10**, 475 (1983)
N.A. Tsyganenko, Global quantitative models of the geomagnetic field in the cislunar magnetosphere for different disturbance levels. Planet. Space Sci. **35**, 1347 (1987)
B.A. Tverskoi, Magnetosphere-ionosphere interaction and polar auroras. Sov. Phys. Usp. **26**, 383 (1983)
E. Tyler, C. Cattell, S. Thaller, J. Wygant, C. Gurgiolo, M. Goldstein, C. Mouikis, Partitioning of integrated energy fluxes in four tail reconnection events observed by Cluster. J. Geophys. Res. Space Phys. **121**, 11798 (2016)
M.E. Usanova, I.R. Mann, J. Bortnik, L. Shao, V. Angelopoulos, THEMIS observations of electromagnetic ion cyclotron wave occurrence: dependence on AE, SYMH, and solar wind dynamic pressure. J. Geophys. Res. **117**, A10218 (2012)

A. Vaivads, M. Andre, S. Buchert, A.I. Eriksson, A. Olsson, J.-E. Wahlund, P. Janhunen, G. Marklund, L.M. Kistler, C. Mouikis, D. Winningham, A. Fazakerley, P. Newell, What high altitude observations tell us about the auroral acceleration: a Cluster/DMSP conjunction. Geophys. Res. Lett. **30**, 1106 (2003)

V.M. Vasyliunas, Mathematical models of magnetospheric convection and its coupling to the ionosphere, in *Particles and Fields in the Magnetosphere*, ed. by B.M. McCormac (D. Reidel, Dordrecht, 1970), p. 60

Z. Voros, W. Baumjohann, R. Nakamura, M. Volwerk, A. Runov, T.L. Zhang, H.U. Eichelberger, R. Treumann, E. Georgescu, A. Balogh, B. Klecker, H. Reme, Magnetic turbulence in the plasma sheet. J. Geophys. Res. **109**, A11215 (2004)

Z. Voros, W. Baumjohann, R. Nakamura, A. Runov, M. Volwek, T. Takada, E.A. Lucek, H. Reme, Spatial structure of plasma flow associated turbulence in the Earth's plasma sheet. Ann. Geophys. **23**, 13 (2007)

T.-H. Watanabe, Feedback instability in the magnetosphere-ionosphere coupling system: revisited. Phys. Plasmas **17**, 022904 (2010)

T.-H. Watanabe, A unified model of auroral arc growth and electron acceleration in the magnetosphere-ionosphere coupling. Geophys. Res. Lett. **41**, 6071 (2014)

T.-H. Watanabe, S. Maeyama, Unstable eigenmodes of the feedback instability with collision-induced velocity shear. Geophys. Res. Lett. **45**, 10043 (2018)

K. Watanabe, T. Sato, Geophys. Res. Lett. **15**, 717 (1988)

T. Watanabe, H. Oya, K. Watanabe, T. Sato, Comprehensive simulation study on local and global development of auroral arcs and field-aligned potentials. J. Geophys. Res. **98**, 21391 (1993)

T. Watanabe, H. Oya, K. Watanabe, T. Sato, Correction. J. Geophys. Res. **99**, 6151 (1994)

T.-H. Watanabe et al., Generation of auroral turbulence through the magnetosphere-ionosphere coupling. New J. Phys. **18**, 125010 (2016)

C.E.J. Watt, R. Rankin, Do magnetospheric shear Alfvén waves generate sufficient electron energy flux to power the aurora? J. Geophys. Res. **115**, A07224 (2010)

C.Q. Wei, B.U.O. Sonnerup, W. Lotko, Model of the low-latitude boundary layer with finite field-aligned potential drops and nonconstant mapping factors. J. Geophys. Res. **101**, 21463 (1996)

D.R. Weimer, C.K. Goertz, D.A. Gurnett, N.C. Maynard, J.L. Burch, Auroral zone electric fields from DE 1 and 2 at magnetic conjunctions. J. Geophys. Res. **90**, 7479 (1985)

J.M. Weygand, M.G. Kivelson, K.K. Khurana, H.K. Schwartzl, S.M. Thompson, R.L. McPherron, A. Balogh, L.M. Kistler, M.L. Goldstein, J. Borovsky, D.A. Roberts, Plasma sheet turbulence observed by Cluster II. J. Geophys. Res. **110**, A01205 (2005)

M. Wiltberger, V. Merkin, J.G. Lyon, S. Ohtani, High-resolution global magnetohydrodynamic simulation of bursty bulk flows. J. Geophys. Res. Space Phys. **120**, 4555 (2015)

S. Wing, J.R. Johnson, P.T. Newell, C.-I. Meng, Dawn-dusk asymmetries, ion spectra, and sources in the northward interplanetary magnetic field plasma sheet. J. Geophys. Res. **110**, A08205 (2005)

S. Wing, S. Ohtani, J.R. Johnson, M. Echim, P.T. Newell, T. Higuchi, G. Ueno, G.R. Wilson, Solar wind driving of dayside field-aligned currents. J. Geophys. Res. **116**, A08208 (2011)

A.N. Wright, W. Allan, Simulations of Alfvén waves in the geomagnetic tail and their auroral signatures. J. Geophys. Res. **113**, A02206 (2008)

J. Wu, D.J. Knudsen, D.M. Gilles, E.F. Donovan, J.K. Burchill, Swarm observation of field-aligned currents associated with multiple auroral arc systems. J. Geophys. Res. **122**, 10145 (2017)

J.R. Wygant, A. Keiling, C.A. Cattell, M. Johnson, R.L. Lysak, M. Temerin, F.S. Mozer, C.A. Kletzing, J.D. Scudder, W. Petersen, C.T. Russell, G. Parks, M. Brittnacher, G. Germany, J. Spann, Polar spacecraft based comparisons of intense electric fields and Poynting flux near and within the plasma sheet-tail lobe boundary to UVI images: an energy source for the aurora. J. Geophys. Res. **105**, 18675 (2000)

A.G. Yahnin, V.A. Sergeev, B.B. Gvozdevsky, S. Vennerstrom, Magnetospheric source region of discrete auroras inferred from their relationship with isotropy boundaries of energetic particles. Ann. Geophys. **15**, 943 (1997)

A.G. Yahnin, V.A. Sergeev, B.B. Gvozdevsky, S. Vennerstrom, Reply. Ann. Geophys. **17**, 42 (1999)

J. Yang, R.A. Wolf, F.R. Toffoletto, S. Sazykin, RCE-E simulation of substorm growth phase are associate with large-scale adiabatic convection. Geophys. Res. Lett. **40**, 6017 (2013)

L.M. Zelenyi, R.A. Kovrazkhin, J.M. Bosqued, Velocity-dispersed ion beams in the nightside auroral zone: AUREOL 3 observations. J. Geophys. Res. **95**, 12119 (1990)

L.M. Zelenyi, E.E. Grigorenko, A.O. Fedorov, Spatial-temporal ion structures in the Earth's magnetotail: beamlets as a result of nonadiabatic impulse acceleration of the plasma. JETP Lett. **80**, 663 (2004)

Y. Zhang, H. Matsumoto, H. Kojima, Whistler mode waves in the magnetotail. J. Geophys. Res. **104**, 28633 (1999)

S. Zou, L. Lyons, C.-P. Wang, A. Boudouridis, J. Ruohoniemi, P. Anderson, P. Dyson, J. Devlin, On the coupling between the Harang reversal evolution and substorm dynamics: a synthesis of SuperDARN, DMSP, and IMAGE observations. J. Geophys. Res. **114**, A01205 (2009)